

Optimal Positioning of the Extended Tail pipes for Liquid Removal from Gas Wells

By
Samuel Amusa

A Thesis Submitted to the
Faculty of Aerospace Engineering TU Delft in partial fulfillment
of the requirement for the degree of Master of Science

27/05/2009
Royal Dutch Shell, Rijswijk the Netherlands

Examination Committee:

Prof. Dr. ir. P.G. Bakker
Dr. B.W. van Oudheusden

Prof. Dr. ir. J.D. Jansen
Dr. P. Oudeman

Abstract

Optimal Positioning of the Extended Tail Pipes for Liquid Removal from Gas Wells

Gas wells usually produce natural gas carrying liquid water or condensate in the form of mist. As the gas flow velocity in the well drops due to the reservoir pressure depletion, the lifting capacity of the gas decreases. When the gas velocity drops to a critical level, liquids begin to accumulate in the well. The accumulation of liquids increases hydrostatical pressure drop which reduces gas-production rate. Low gas production rate will cause gas velocity to drop even further. Eventually, the well will produce in bubbly flow regime and cease producing. This phenomenon is referred to as liquid loading.

One of the most effective remedies commonly applied to minimize liquid loading impact on gas production is to place an extra tube with small diameter at the bottom end of production tubing. By reducing the flow area, the hanging tail pipe increases gas velocity and transport the accumulated liquid in the well to surface.

The disadvantage of the extended tail pipes (which is also referred to as velocity string in the industry) is the increase in frictional pressure drop which will also tend to constrain production. Hence the optimal setting depth and diameter of the tail pipe are required, such that liquid is removed and production is maximized.

Through this project work, liquid loading behavior was modeled and a computational algorithm was developed to solve the fluid flow model numerically. Apart from the optimum tubing size which can be determined through the developed fluid flow model, the factor that contributes to the effectiveness use of tail pipe was also discovered.

The developed fluid flow model can be developed further into a tool that for analyzing wellbore performance.

Preface

This report was written in partial fulfilment of the requirement for master degree of science in Aerospace Engineering, TU Delft. I took up an assignment with *In well Modelling team*- a sub-group within exploration and production stream in Royal Dutch Shell, Rijswijk the Netherlands.

I would like to express my sincere gratitude to my leading supervisor in Shell Dr. Piet Oudeman. Without his unique support this thesis would not have become a reality. He had been instrumental to me in the course of this project. I am grateful for his willingness in sharing his invaluable experiences with me. I would also like to thank my university supervisor Prof. Dr. J.D. Jansen for his time and helpful critique he offered in the course of this project. In Particular, I am deeply indebted to him for his ideas which he shared with me through his earlier research project work: ‘Numerical modeling of flow in extended stringer completions’.

My thanks also go to Prof. Bakker for allowing me to undertake this insightful project with Shell and the oversight he provided for the project. I am also indebted to Dr. Veldhoeven for recommending me for this project. Thanks very much.

I would like to thank Jiri Beran, Murat Kareem and Gbenro Oguntimehin for their time and energy they offered me during my stay in Shell. I am delighted with all the meaningful discussions we had together.

I wish to express my thanks to my family back home in Nigeria, my parents, siblings, my wife Damilola and my dear friend Henry. I am indebted to their unwavering moral support and encouragement.

Finally, my greatest thank goes to the Almighty God Jehovah, for the gift of life he gave me and the means through which He sustains me.

SUMMARY

Gas wells producing late in their life are normally subject to liquid loading problems. As rates fall below the critical rate necessary for unloading, a static column will often develop in the well. This can result from condensed water out of the gas phase or formation water being produced into a well having insufficient gas velocity to clear the liquid from the wellbore. The presence of this liquid column impairs the well performance by imparting additional back pressure on the reservoir. This phenomenon is referred as liquid loading in gas wells.

Several measures can be taken to solve the liquid-loading problem. Foaming the liquid water can enable the gas to lift water from well. Wellhead Gas Compression is another technique, by which the tubing head pressure is reduced, and thereby increases gas velocity to lift the liquids to surface. Using smaller tubing or creating a lower wellhead pressure sometimes can maintain mist flow.

The problem with the use of smaller tubing (which is also referred to as velocity string in the industry) is that, the smaller the tubing diameter size the greater the friction introduced by the tubing. And friction limits production. Setting the velocity string deeper through the perforations depth increases the potential to increase production rate. However, as the velocity string gets deeper in the wellbore the fluid flow exposes to a larger contact area in the pipe thereby increases energy required to overcome frictional pressure. Increase in energy required to overcome frictional pressure will increase bottomhole pressure and therefore curtails the gas inflow capacity. Production will be reduced.

The focus of this project work is to design velocity string size in such a way that the effect of friction on production is minimized and gas velocity is increased. Increase in gas velocity would transport the liquid accumulated downhole to surface. If the design of velocity is properly done liquid loading could be minimized and production would be maintained.

A fluid flow model was developed to replicate liquid loading phenomenon. This fluid flow module consists of systems of differential equations, which are non-linear. Gas inflow from reservoir was modeled as a single-phase flow by using Rawlins& Schellardt gas flow equation. Gray correlation was used for calculating pressure drop in the casing, velocity string and in production tubing. We do not include separate liquid influx in the inflow analysis. We assumed that the source of liquid in the flow stream is due to gas condensation in the wellbore. As the pressure and temperature change downhole, condensation will occur, thereby creating stagnant liquid in the wellbore bottom end. We prescribed boundary conditions to complete the solution of the system of differential equations. The complete set of the systems of differential equations will be too difficult to solve analytically owing to the complexity of the module equations, furthermore there

exist some complicated function in the module equations, which cannot be solved explicitly. In addition, it appears that the boundary value problem is multi-boundary problem, which requires specification of boundary conditions in three different parts. Thus using a numerical method eases the problem solving technique. Runge-Kutta numerical scheme was used in solving the discretized flow equations. The wellbore system was partitioned into segments. Doing that enables variation of the optimization parameters in relation to the wellbore geometry.

A problem scenario was used to study the effect of the optimizations parameters – namely the depth and diameter of a velocity string. It is revealed that the optimal depth location lies between $\frac{1}{2}$ and $\frac{3}{4}$ way depth of perforated section of the wellbore. It is further revealed that the performances of velocity string declines rapidly when placed close to bubbly or slug flow regime.

The selection of optimal diameter size was done by using nodal analysis. Among factors considered were the differences between critical gas rate and operating gas rate for a given diameter size and differences in the nodal pressure for each selected candidate. Through a case scenario used to study the effectiveness of the module in optimizing velocity string, it was revealed that when a wellbore is completed with an optimized velocity string, gas production rate is increased by 26%.

Recommendations for further study were proposed especially in the area downflow pressure module. Homogeneous model approach was used to determine liquid hold up for downflow pressure gradient. There is a concern over the accuracy of the pressure value estimation. Although the approach used is in line with prevailing methods proposed in literature. The other aspect that calls for further analysis is the inclusion of transient module in the module formulation. The transient analysis can give information about time it will take to de-liquify a well and for how long does a selected candidate tubing size will remain effective before re-completion take place.

Table of Contents

SUMMARY	4
LIST OF FIGURES AND TABLE	7
1.0. INTRODUCTION	8
1.1. Objectives and Scope	9
1.2. Approach to Solution	9
1.3. The Report Outline	10
2.0. BACKGROUND INFORMATION	11
2.1. Historical Background of Liquid Loading	11
2.2. Multiphase flow	15
2.2.1. Transition in flow regimes of a liquid loaded well	16
2.3. Source of Liquids in a Producing Gas Well	17
2.4. Pressure drop model	17
2.4.1. Gray Correlation	18
2.4.2. Friction factor	21
2.5. Multiphase Downward Flow	23
2.6. Nodal Analysis	24
3.0. MODELING FLUID FLOW	25
3.1. Geometrical Description	25
3.1.1. Geometric relation	27
3.2. Modeling of gas production	30
3.2.1. Inflow Modeling	31
3.2.2. Outflow Modeling	34
3.3. Setting up Boundary conditions	35
3.3.1. Casing-Velocity String Annulus - Boundary conditions	35
3.3.2. Velocity String-Tubing Strings- Boundary conditions	36
3.4. Estimation of pressure in the wellbore	38
3.4.1. The Down flow Pressure Gradient	41
3.5. Model Equations	42
4.0. NUMERICAL ANALYSIS	45
4.1. Numerical scheme representation	45
4.2. Flow chart for computational algorithm of fluid flow model	47
5.0. RESULTS & DISCUSSION	50
5.1. Example Calculations	50
5.2. Velocity string Optimal Depth	50
5.3. Selection of Optimum Diameter Size	52
6.0. CONCLUSION AND RECONMENDATIONS	55
REFERENCES	56
NOMENCLATURE	58
APPENDIX B: Computer code	60

LIST OF FIGURES AND TABLE

Figure 2.1: Example of a typical production response in liquid loading gas well (figure taken from Royal Dutch Shell report EP 2003-5307 p.3).....	12
Figure 2.2: Illustration of Critical concept (courtesy of Lea J., Nickens, H., Wells, M)..	13
Figure 2.3: Multiphase flow regimes in vertical conduit.....	16
Figure 2.4: Changing behavior of a liquid loaded well	16
Figure 2.5: Single-phase and multiphase flows through upward and downward pipe sections.....	23
Figure 2.6: Illustration of Nodal analysis	24
Figure 3.1: Illustrative representation of a Wellbore.....	26
Figure 3.2: Schematic representation of the wellbore system.....	26
Figure 3.3: Velocity String variations.....	28
Figure 3.4: Example of Gas flow rate vs. non-dimensional length.....	29
Figure 3.5: Schematic of vertical well, showing gas inflow.....	32
Figure 3.6: Perforated section of the Wellbore.....	35
Figure 3.7: Velocity String - Production Tubing String completion.....	37
Figure 3.8: Illustrated Pressure profiles in the wellbore.....	40
Figure 3.9: Wellbore representation.....	43
Figure 4.1: Grid representation of the wellbore.....	47
Figure 4.2: An illustrated example of unmatched pressure profiles.....	48
Figure 4.3: Flowchart for computation algorithm.....	49
Figure 5.1: Pressure Traverse.....	51
Figure 5.2: Wellbore pressure along the perforated section.....	51
Figure 5.3: Flow rate vs. setting depth.....	52
Figure 5.4: Nodal Analysis.....	53
Figure 5.5: Velocity profiles along the wellbore.....	54
Table 5.1: Presentation of the Nodal results for different diameter sizes.....	533

1.0. INTRODUCTION

Many gas wells that have been in operation for many years decline in volume of gas they produce due to decline in their reservoir pressure. Hydrocarbon condensates or free liquid water from the reservoir are usually co-produced with natural gas to the surface when there is sufficient reservoir energy. But, with depletion of reservoir pressure, there comes a time when liquids can no longer be lifted to the surface by the flowing gas and they begin to accumulate in the bottom of the well, dramatically inhibiting or stopping gas production. This accumulation of liquids in the bottom of the gas well is termed as liquid loading. Accumulation of liquids in the bottom of a gas well increases backpressure on reservoir and therefore further reduces gas production rate. Low gas production rate will cause gas velocity to drop further. Eventually, the well will produce in the bubbly flow regime and cease producing.

Liquid loading usually starts in the casing below the end of production tubing where the cross-sectional area is relatively larger, and the velocities are correspondingly smaller than in tubing. One of the most commonly applied remedies to liquid loading problem is by reducing the flow area with the intension to increase the gas flow velocity. Increasing the gas flow velocity will increase lifting capacity of the gas thereby removing the accumulated liquid and restore it to surface. Hanging a small ID tail pipe at the production-tubing shoe is one of the viable options often used in oil and gas industry in combating liquid loading problem. This extended tail pipe is sometime referred to as a velocity string. The tail pipe is named velocity string due to the fact that the tail pipe or stinger increases gas velocity.

The main drawback of the velocity string is the introduction of frictional flow resistance in the well. Therefore the price for suppressing liquid loading is the decreased in gas production. This makes selection of the optimum size of the velocity string critical. An optimal velocity string has to be selected such that liquid loading is delayed over a long period and at the same time maintaining the highest possible production.

The usefulness of velocity string in combating liquid loading underscores the need for its optimization. There are basically two parameters that require optimization work namely:

- The optimal depth at which the velocity string is placed.
- The optimal diameter of the velocity string.

It is expected that the determination of the above mentioned parameters would increase the gas volume flow rate from a liquid loaded gas well and thereby improve the recovery factor.

1.1. Objectives and Scope

The objectives of this project are

- To develop a procedure for design optimization of a velocity string
- To determine optimal setting depth of velocity string in gas wells
- To determine optimal diameter for velocity string tubing
- To determine the factors that influence the optimization constraints

1.2. Approach to Solution

The solution to the optimization problem being considered can be approached in various ways. The common methods often used in oil and gas industry for analyzing and predicting fluid flow problem that concerns multiphase flow can be rightly grouped into three categories:

- (1) **Experimental method:** A phenomenon is tested through a laboratory-sized model and equipped with appropriate instrumentation.
- (2) **Computational method:** This involved using mathematical or empirical equations models for the fluid flow and solved the equations numerically with computers.
- (3) **Field test:** This is a reality test. It involves taking measurement samples from field and process the data collected to derive information about phenomenon being investigated.

Sometimes, all the three above-mentioned methods are used together or supplement each other in order to find solution to a problem.

It is possible to use a full-scale/small size laboratory model and then extrapolated the scale prototype data by a reliable theoretical or computational model. The disadvantage of this method however is that the predictive capability, reliability and physical understanding must rely heavily on theoretical and/or computational models used for extrapolation. That is where the complexity of most multiphase flows presents a major hurdle.

Carrying out field test could have been the best approach to get accurate answers about the subject matter. Conducting field test requires phenomenal resources. Given that liquid loaded well is already operating on the edge of profitability due to their low productivity, it is more economically practical to look for means that do not require substantial resources to carry out the optimization work.

Although there are also justifications for using sophisticated approach in solving the optimization problem. From practical point of view the approach to be used for this work is by developing fluid flow models and simulated it on a computer. Apart from the fact that it requires fewer resources to implement computational fluid flow solution; all the

necessary model equations are already available. To solve the fluid flow problem will require *discretizing* wellbore into elemental segments and solve fluid flow equations on each elemental node. The inflow from reservoir will be coupled with vertical wellbore. The fluid flow will be modeled to allow for accumulation of liquids downhole, hence replicating liquid loading phenomenon. From the model, it is expected to see how velocity string depth varies with gas volumetric flowrate. The depth at which maximum flowrate is achieved would be considered as the optimum depth. By comparing the outflow performance- that is the ability of the conduit to transport fluid to surface, with the inflow performance – that is the ability of the reservoir to deliver, the optimum diameter can be determined. The later approach is called nodal analysis.

1.3. The Report Outline

The outline to this report is as the follows: In chapter two the background information about liquid loading phenomenon is presented. We start with the genesis of liquid loading problem, classification of flow regime, what problem caused by liquid loading and the dynamic behavior of liquid loading in gas wells. The background information presented in chapter two is aimed at introducing liquid loading in gas wells to those readers that have no previous knowledge of this research work and at the same time creating groundwork upon which fluid flow model in chapter three is based upon. Discussions on the description of fluid flow properties that aids transport phenomena in the wellbore are presented also in chapter three.

The fluid flow models developed in chapter three happened to be in non-linear system of differential equations and there is implicit relationship among the fluid properties. Therefore, analytic solution to these model equations is not possible and we must resort to a numerical solution. Chapter four therefore, presents the numerical analysis to the solution. A Flow-chart that aids the implementation of computational algorithm on a computer is also presented in chapter four.

In chapter five, we simulated a problem scenario. The results show where optimal depth lies in the wellbore. Through the chapter, the modus operandi that guides the use and design of velocity string are presented. The conclusion and recommendations are made in chapter six. The area for further research and improvement is highlighted whilst creating groundwork for implementation.

2.0. BACKGROUND INFORMATION

This chapter is meant to present the fundamental information on liquid loading process in the gas well. The fundamental information will include discussion about different flow regimes and the process a gas well may undergo before it is killed by accumulated liquid.

2.1. Historical Background of Liquid Loading

The phenomenon of liquid loading in gas wells became apparent in the 1940's in the USA, when gas well operators were required to report to the regulating authorities on the production potential of their gas wells. In wet gas wells, it was however observed that often time the calculated flowing bottomhole pressure for the lowest rates did not fit the inflow performance curve as derived from high rate test points. Other problems realized were instability of flowing head pressure and difficulties in obtaining representative liquid sample.

These problems were seen to be caused by the presence of liquids in the well, which were not transported to surface in a steady continuous mode. At the lowest test rates the gas velocity was insufficient to carry liquids to surface either in the form of droplets or as a liquid film on the tubing wall. The concept of critical velocity was introduced to predict onset of liquid loading. It is believed that when gas velocity is below the critical velocity liquid loading is imminent. Figure 2.1 shows an example of a gas well that initially producing steadily. After couple of years the gas productions start declining. As the gas volumetric flowrate decline the liquid production rate starts increasing.

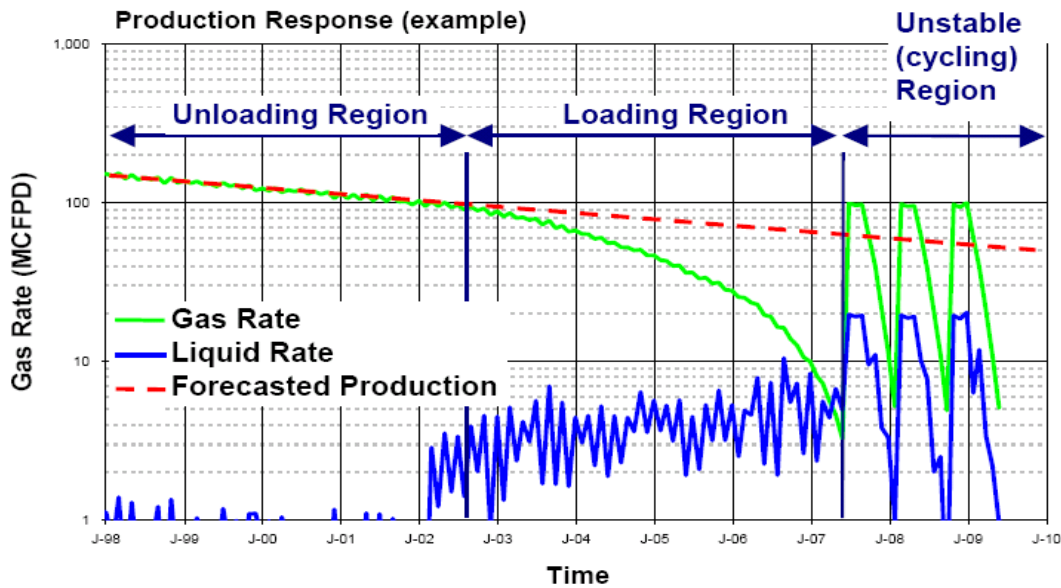


Figure 2.1: Example of a typical production response in liquid loading gas well (figure taken from Royal Dutch Shell report EP 2003-5307 p.3).

The production becomes unstable and eventually the well will die. Liquid removal from the well will cause resurgence of gas production. Thus the ability to determine when gas rate is below critical velocity was considered instrumental for combating the problem of liquid accumulation downhole.

The first approach to solve these problems was developed by Duggan¹ who postulated that the gas velocity at wellhead should not be less than 15 ft/s (4.572m/s) at the lowest test rate. Although the approach worked in a number of cases, it was often felt to be conservative and the criterion could not be adhered to for e.g. low rate producers of which the well head velocity was already close to 15 ft/s at full flow.

A more refined approach was presented by Turner *et al*². Turner *et al*² were the first investigators to develop mathematical model for analyzing and predicting the minimum gas-flow rate to prevent liquid loading. They postulated two mathematical models to describe the liquid loading problem, one is the film-movement model and the other one is entrained drop-movement model. On the basis of analyses of field data, they concluded that the film movement model does not represent the controlling liquid –transport mechanism. This was because the velocity predicted to sustain liquid transported as a film coating the tubing wall to the surface is high which can only be applicable to high rate producers. Since at low gas rate liquid are still being transported to the surface, the conclusion to this realization was that liquid film transport mechanism can not be valid approach to predict minimum gas velocity required to continuously transport liquid droplets to surface.

The entrained liquid drop-movement model approach was developed on the basis of the critical velocity of liquid drops and the maximum drop diameter corresponding to the critical Weber number of 30. In this model, the droplet weight acts downward, and the

drag force from the gas acts upward (Figure 2.2). When the drag is equal to the weight, the gas velocity is at "critical." Theoretically, at the critical velocity or terminal velocity, the droplet would be suspended in the gas stream, moving neither upward nor downward. Below the critical velocity, the droplet falls, and liquids accumulate in the wellbore.

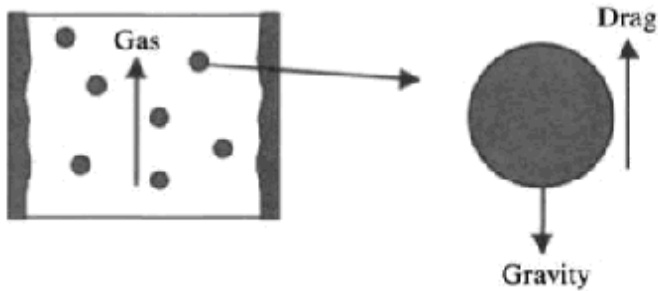


Figure 2.2: Illustration of Critical concept (courtesy of Lea J., Nickens, H., Wells, M)

Turner's mathematical liquid droplet model criterion expressed in equation 2.1 expressed in U.S. field units as:

$$v_c = \frac{1.3\sigma_l^{1/4}(\rho_l - \rho_g)^{1/4}}{C_d^{1/4}\rho_g^{1/2}} \quad (2.1)$$

v_c - Critical velocity [ft/s]

σ_l - Gas-liquid interfacial tension [dyne/cm]

ρ - Densities of gas and liquid at wellhead conditions [lb/ft³]

C_d - Drag coefficient [-], recommended a value 0.44.

The Turner *et al*² is based on Weber number which relates inertia force and surface tension force and is defined mathematically as:

$$N_{we} = \frac{\rho v_g d_p}{g_c \sigma} \quad (2.2)$$

where

N_{we} - Weber number [-]

v_g - *In situ* gas velocity [ft/s]

ρ - Density [lb/ft³]

d_p - Liquid droplet diameter [ft]

g_c - Gravitational constant [lbm-ft/lbf-s²]

σ - Interfacial (surface) tension between liquid and gas

According to Turner et al., gas will continuously remove liquids from the well until its velocity drops to below the critical velocity. The minimum gas flow rate for a particular set of conditions (pressure and conduit geometry) can be calculated using equations (2.1) and (2.3)

$$Q_{gm} = \frac{3.06 p v_{sl} A}{T z} \quad (2.3)$$

Where

Q_{gm} - The minimum required gas flow for liquid removal [MMscf/day]

p - Pressure at depth of interest [psia]

A - Cross-sectional area of conduit, [ft²]

T - Temperature [°R]

z - Gas compressibility factor

Turner *et al.* found that this entrained drop movement model underestimates the minimum gas flow rates. They recommended that the equation-derived values be adjusted upward by approximately 20 % to ensure removal of all drops. The 20% adjustment is to account not only for the slip velocity, but also for the fact that the minimum gas velocity required for transporting the liquid droplets upward is the sum of the droplets (i.e. slip velocity) in the flow stream and the transport velocity of the droplets.

Turner *et al.* believed that the discrepancy was attributed to several facts including the use of drag coefficients for solid spheres, the assumption of stagnation velocity, and the critical Weber number established for drops falling in air, not in compressed gas.

Numerous investigators³⁻⁴ have refined the Turner et al basic model given in equation 2.1. One of the refinements of the Turner's expression was found by Kutateladze⁴ who studied flooding in two-phase systems:

$$v_c = 3.1 \frac{g^{1/4} \sigma_l^{1/4} (\rho_l - \rho_g)^{1/4}}{\rho_g^{1/2}} \quad (2.4)$$

v_c - Critical velocity [ft/s]

σ_l - Gas-liquid interfacial tension [dyne/cm]

ρ - Densities of gas and liquid at wellhead conditions [lb/ft³]

g - Gravitational acceleration [ft/s²]

In eighties the North West European gas well operators realized that none of the expressions for critical velocities predicts that the well will not flow once the well head velocity has declined to the values predicted by these module equations²⁵. That was why

they called for improved prediction of overall wet gas well performance rather than just the point where liquid transport ceased to be continuous. Among many modification put in place is the use of Kutateladze's expression as a critical velocity imbibed in Gray correlation module. Discussion about Gray correlation is presented in section 2.4.

2.2. Multiphase flow

The study of the multiphase flows is of major importance in oil and gas industry since it is found quite frequently during production process. The physics involved in these flows is very complex due to interactions between the different phases. In order to deal with this complexity, sophisticated numerical methods with several parameters (most determined from experiments) are required. The way conservation laws are applied in a single-phase flow is not necessarily the same as in multiphase flow. There is no doubt that liquid loading process will be wrongly modeled if quantitative description of single-phase flow is used in description of liquid loading. To understand the effects of liquids in a gas well, we must understand how the liquid and gas phases interact under flowing conditions. Multiphase flow in a vertical conduit is usually represented by four basic flow regimes shown in Figure 2.3. A flow regime is determined by the velocity of the gas and liquid phases and the relative amounts of gas and liquid at any given point in the flow stream.

Bubble Flow—The tubing is almost completely filled with liquid. Free gas is present as small bubbles, rising in the liquid. Liquid contacts the wall surface and the bubbles serve only to reduce the density. Up to circa 30% are in gas volume fraction.

Slug Flow—Gas bubbles expand as they rise and coalesce into larger bubbles and then slugs. Liquid phase is still the continuous phase. The liquid film around the slugs may fall downward. Both gas and liquid significantly affect the pressure gradient.

Slug-Annular Transition—The flow changes from continuous liquid to continuous gas phase. Some liquid may be entrained as droplets in the gas. Although gas dominates the pressure gradient, liquid effects are still significant.

Annular-Mist Flow—Gas phase is continuous, and most of liquid is entrained in the gas as a mist. Although the pipe wall is coated with a thin film of liquid, the pressure gradient is determined predominately from the gas flow.

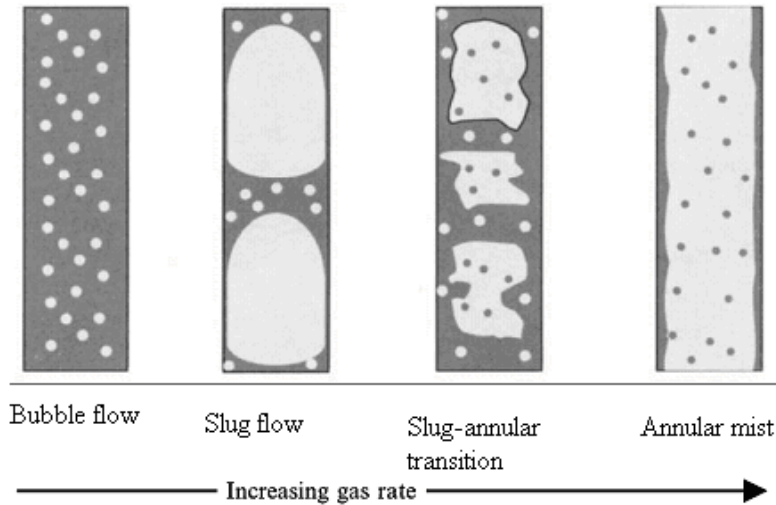


Figure 2.3: Multiphase flow regimes in vertical conduit

One or more of these regimes will be present at any given time in a well's history.

2.2.1. Transition in flow regimes of a liquid loaded well

During a lifetime of a gas well, it may go through all flow regimes described in above. What determines type of flow regime is the velocity or flow rate. Figure 2.4 shows an illustration of a typical gas well how it progresses from an initial production to end of life.

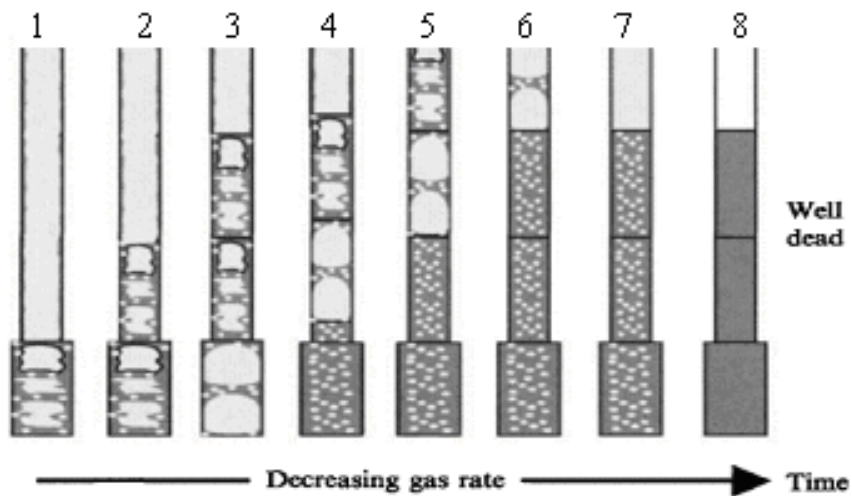


Figure 2.4: Changing behavior of a liquid loaded well

In this illustration, it is assumed that the tubing end does not extend to the mid-perforations so that there is a section of casing from the tubing end to mid-perforations. The well underwent eight stages before it finally dead.

At stage

- (1) The well has a high rate so that the flow regime is in mist flow in the tubing; however, it may be in bubble, transition, or slug flow below the tubing end to the mid-perforations.
- (2) At this stage the production declines in time.
- (3) The liquid production has started increasing, the flow regimes from the mid of perforation to the halfway of the conduit may be in slug or bubble flow regime. But the flow condition at the surface still exhibits mist flow.
- (4) Liquid is taking more prominent space in the flow regime and flow rate declines further.
- (5) Downhole the flow regime has completely turned to bubble flow. The flow at the surface in transition state, exhibiting instability.
- (6) This transition is further accompanied by a marked increase in the decline rate.
- (7) The flow regime further downhole may be in bubble or slug flow, even though the surface production is in stable mist flow.
- (8) Eventually, the unstable slug flow at surface will transition to a stable, fairly steady production rate again as the gas rate declines further. This event occurs when the gas rate is too low to carry liquids to surface and simply bubbles up through a stagnant liquid column.
- (9) At this stage the well practically dead. However, if corrective action is taken to rescue the situation the well can still resurrect.

It is also possible that the well may continue to flow for a long period in a loaded condition and that gas produces up through liquids with no liquids rising to the surface.

2.3. Source of Liquids in a Producing Gas Well

Many gas wells produce not only gas but also condensate and water. If the reservoir pressure has decreased below the dew point, the condensate is produced with the gas as a liquid; if the reservoir pressure is above the dew point, the condensate enters the wellbore in the vapor phase with the gas and condenses as a liquid in the tubing or separator. Produced water may have several sources. Water may be coned in from an aqueous zone above or below the producing zone. If the reservoir has aquifer support, the encroaching water will eventually reach the wellbore. Water may enter the wellbore from another producing zone, which could be separated some distance from the gas zone. Free formation water may be produced with the gas. Water and/or hydrocarbons may enter the wellbore in the vapor phase with the gas and condense out as a liquid in the tubing.

2.4. Pressure drop model

In order to estimate the absolute open flow potential of a gas well, it is necessary to determine the static and flowing bottom-hole pressures. This is done either by actual

measurement with bottom-hole pressure gauge, or by calculation using wellhead pressure measurements. The motivation of this section is to present a reliable pressure drop module for subsequent computation in wellbore for gas/condensate systems. The accurate predictions of the flowing bottomhole pressure (FBHP) for various operating conditions are needed for analysis of gas wells producing with or without some liquid production. Later in the gas well's life, an operating condition often encountered is that of liquid loading although low production rates, high surface pressures, and large tubing can contribute to liquid loading at any time. Several multiphase flow correlations are available in literature, which can predict pressure traverses when flowing fluid is gas and liquids. By comparing measured data to predictions from the Gray⁵ correlation and the other correlations Kumar⁴ concluded that Gray correlation is the best correlation for gas wells producing some liquids. This conclusion was made by comparing twelve widely used correlations in industry (Cullender and Smith⁶, Poetman and Carpenter⁷, Baxendell and Thomas⁸, Fancher and Brown⁹, Duns and Ros¹⁰, Orkiszewski¹¹, Beggs and Brill¹⁸, Duckler¹³ *et. al*, Mukherjee and Brill, Aziz¹⁵, Govier and Forgarsi, and original Gray correlations⁵). The original Gray correlation is a two-phase vertical flow correlation for gas wells to determine pressure gradients with depth that produce limited amount of condensate fluid or water. The limits on water and condensate in the original data set to which Gray compared his model were 10 bbl-water /Mmscf/D and 150 bbl- condensate/ Mmscf scf/D. His model was correlated against 108 well test data sets.

2.4.1. Gray Correlation

Gray stated that that the equation for steady state, vertical, two-phase flow for compressible fluid is:

$$\frac{dp}{dz} = g \left(\alpha \rho_g + (1 - \alpha) \rho_l \right) + \frac{f_t \rho_m V_m^2}{2D} + \rho_m V_m \frac{dV_m}{dz} \quad (2.5)$$

Where (in any consistent unit system)

D - Hydraulic diameter [m]

f - Fanning friction factor [-]

V_m - Mixture velocity [m/s]

α_g - In situ gas fraction (gas hold-up); [-]

$\rho_{g,l}$ - Gas, Liquid densities [kg/m³]

ρ_m - Mixture density [kg/m³]

The Gray correlation utilizes the following dimensionless parameters:

$$N_v = \frac{\rho_m^2 V_m^4}{g \sigma (\rho_l - \rho_g)} \quad (2.6)$$

$$N_D = \frac{g(\rho_l - \rho_g)D^2}{\sigma} \quad (2.7)$$

$$R = \frac{V_{so} + V_{sw}}{V_{sg}} \quad (2.8)$$

where

$V_{so,w,g}$ -Oil, Water, Gas superficial velocity

Superficial velocity is the velocity of when phase would be only one in the pipe. The velocity number N_v is the square of what is known as the Kutateladze number that is used in annular-mist flow regime modeling or to describe the hanging film phenomenon. N_d is the diameter or Bond number which indicates the ratio (gravitational force) / (surface tension force) and is used in momentum transfer in general and motion of bubbles and droplets calculations in particular. The parameter R is a dimensionless liquid to gas ratio.

Gas hold-up α_g is an important parameter in a two-phase flow. It is the ratio of the volume of a pipe segment occupied by gas to the volume of the pipe segment. Summation of gas and liquid hold-ups α_l is unity.

$$\alpha_g + \alpha_l = 1 \quad (2.9)$$

In Gray correlation special attention is given to the formulation of gas hold-up. Since its accuracy will largely affect pressure gradient estimation. The gas hold-up is expressed as follows:

$$A = 0.0814 \left(1 - 0.554 \ln \left(1 + \frac{730R}{R+1} \right) \right)$$

$$B = -2.2314 \left(N_v \left(1 + \frac{250}{N_d} \right) \right)^A$$

$$\alpha_g = \frac{1 - \exp^B}{R + 1} \quad (2.10)$$

The estimation of mixture surface tension is obtained as:

$$\sigma_m = \frac{q_o \sigma_o + 0.617 q_w \sigma_w}{q_o + 0.617 q_w} \quad (2.11)$$

$$\sigma_w = (2.115 - 0.119 p) (0.174 - 2.09 * 10^{-4} (T - 460)) \quad (2.12)$$

$$\sigma_c = 0.044 - 1.3 * 10^{-4} (T - 460) \left(\frac{p_d - p}{p_d - 2120} \right)^{2.5} \quad (2.13)$$

where

p_d - Dew point pressure [psi]

T - Temperature ($^{\circ}$ R)

$\sigma_{m,w,c}$ - Mixture, Water, Condensate surface tension [lbm/s²]

Modification to the original Gray correlation came when it was discovered that the correlation failed to predict pressure drop accurately when gas production rates is low and liquid ratio is high i.e. gas production less than 140 000 stdm³/d (5MMscf/d) and liquid recovery less than 60 m³/10⁶ stdm³ (10bbl/MMscf). A thorough look at the gas void equation (2.10) shows that when R vanishes-meaning fluid flow is dry gas; the liquid hold-up is expected to vanish either. However, when R is made zero in the equation (2.10) a non-zero hold-up results. To correct the error introduced by under prediction of pressure drops in Gray correlation, the original Gray hold-up was modified by incorporating the Wallis hold-up relation¹⁷ for intermittent flow conditions.

Wallis expression for gas hold-up is calculated as follows:

$$\alpha_g = \frac{R + (-v_b / v_{sg})}{R + 1 + (v_b / v_{sg})} \quad (2.14)$$

With bubble rise velocity v_b experienced by gas which is due to buoyancy is calculated according to:

$$v_b = 0.345 \sqrt{Dg \frac{\rho_l - \rho_g}{\rho_l}} \quad (2.15)$$

where

α_g - In situ gas fraction (gas hold-up) [-]

v_b - bubble rise velocity [m/s]

D - Hydraulic diameter [m]

$\rho_{g,l}$ - Gas, Liquid densities [kg/m³]

R - Liquid/ gas ratio [-]

Comparison with the results of a series of specific field-tests on liquid loading demonstrated that this modification corrected the systematic under prediction of gradients at the lowest flow rates¹⁸.

2.4.2. Friction factor

The determination of the frictional pressure drop is not possible by theoretical analysis alone because the phenomenon of the momentum transfer between the phases, the wall friction and the shear at the phase interface can not be specified quantitatively. In practice, use is, therefore, made up of the relationships based on the models, which are either modified or correlated by means of measurements.

In the present case, Gray correlation uses modified Darcy-Weisbach expression, which assumes the flow to be turbulent

$$\frac{dp}{dz} = f \frac{\rho V^2}{2D} \quad (2.16)$$

Where f is the friction factor $f = 64/Re$, ρ is the fluid density, V stands for fluid velocity of the flow and D stands for pipe diameter.

The wall roughness factor now becomes pseudo wall roughness, which is calculated from an Oosterhout-Weber type correlation³¹. The pseudo wall roughness is combined with a Colebrook White function, which gives a two-phase friction factor.

Colebrook white function is giving implicitly as:

$$\frac{1}{\sqrt{f}} = -2 \log_{10} \left(\frac{\varepsilon}{3.71D} + \frac{2.51}{N_{RE} \sqrt{f}} \right) \quad (2.17)$$

Where Reynolds number N_{Re_m} is defined as

$$N_{Re_m} = \frac{\rho_m v_m D}{\mu_{av}} \quad (2.18)$$

μ_{av} - Average viscosity of the liquid and gas phase [Pa s].

f - Friction factor [-]

ε - Wall roughness [m]

The pseudo wall roughness is calculated from a van Oosterhout –Weber number type correlation³¹ is modified and bounded to fit field observation as determined from the regression analysis:

$$r = r' = \frac{28.5\sigma}{0.3048\rho_m v_m^2} \quad \text{for } R \geq 0.007 \quad (2.19)$$

$$r = r_g + R \left(\frac{r' - r_g}{0.007} \right) \quad \text{for } R < 0.007 \quad (2.20)$$

$$r \geq 2.77 \times 10^{-5} \quad \text{for } 0 \leq R \leq \infty$$

Where

r – pseudo wall roughness [ft]

r_g – absolute wall roughness for dry gas flow [ft]

R – superficial liquid/gas ratio (in situ) [-]

σ – interfacial tension [lbsm/s²]

ρ_m – mixture density [lbs/in³]

Depending on Weber number, the pseudo wall roughness can be either greater or smaller than dry gas value that is why a limit condition $r \geq 2.77 * 10^{-5}$ ft is used in the correlation. The unit has to be consistent in usage; therefore conversion of unit is often required for use in computation.

The Gray pressure drop correlation was developed with the used of open tube configuration. There is no method developed specifically for tubing-velocity string annular flow configuration. To incorporate annular configuration in the Gray correlations, modification to the method used for tubing strings has to put in placed especially when the phenomenon involves multiphase gas-liquid flow. This is because installation of velocity sting in the flow stream could affect the flow regimes. More so, the interaction between gas and liquid in annular configuration are totally different from those in an open tube configuration. As a result of the perturbation caused by velocity string, quantities such a liquid hold-up and interfacial friction will be affected. And these quantities determine the value of pressure drop in tubing-velocity string annulus.

There are various approaches feasible to adapt the correlation to annular flow. Various models for annular flow equivalent pipe have been reported in the literature¹⁶. There is no consensus amongst industry practitioner as to the most appropriate equivalent pipe diameter relationship to use for annular flow computations to achieve the best accuracy. Oudeman⁴ however, indicated from field test carried out that hydraulic radius models generally provide reasonable and reliable results. Hydraulic diameter is expressed as

$$D_H = \frac{A}{P} \quad (2.21)$$

Where

D_H - Hydraulic diameter [m]

A - Flow Area [m²]

P – Perimeter [m]

In an annulus of two concentric cylinders, the hydraulic diameter between the outer diameter of the inner tube, D_1 , and the inner diameter of the outer tube, D_2 , it can easily be shown that:

$$D_H = D_2 - D_1 \quad (2.22)$$

2.5. Multiphase Downward Flow

Amongst many factors that affect the properties of multiphase flow is the geometry of the flow path. Flow path geometry in return affects the liquid hold up. Liquid hold in return affects pressure drops. This process is illustrated in the figure 2.5.

Pressure drop is fully recovered when fluid flow in upward and downward direction in single phase flow.

As shown in figure 2.5(a), when fluid flows from A to B, the pressure at B is lower than the pressure at A due to the elevation change (pressure loss).

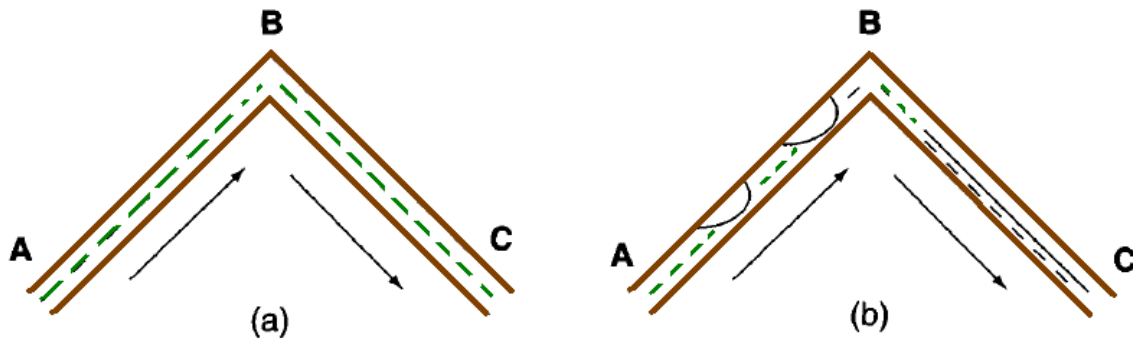


Figure 2.5: Single-phase and multiphase flows through upward and downward pipe sections

But as the flow continues from B to C, the pressure gained at C due to the elevation change is equal to the pressure loss from A to B. Therefore, with single phase flow, the pressure lost in the upward flow can be fully recovered in downward flow. But the same conclusion may not always hold true in gas-liquid two-phase flow. As shown in Figure 2.5 (b), the flow regime in the upward flow section (from A to B) may not be the same as the flow regime in the downward flow section (from B to C). With different flow regimes, the liquid holdup in each section may not be the same. Thus, the pressure loss in the upward flow section may not be fully recovered in the downward flow section.

The implication of this realization is that pressure modules that are used for upward multiphase flow will fail to estimate correct pressure values for downward flow if the physics involved in these flows are not properly accounted for.

2.6. Nodal Analysis

The flowing bottomhole pressure required to lift the fluids up to surface may be influenced by the size of tubing string, choke installed at downhole or surface and pressure loss along the pipeline. To predict performance of a given well, the reservoir inflow performance curve and tubing outflow performance are intersect to get operating point of the well. The combined performances which is known as nodal analysis (see figure 2.6), is often used as tool for optimizing well production and sizing equipment. The analysis method will be used in selecting diameter size of the velocity string.

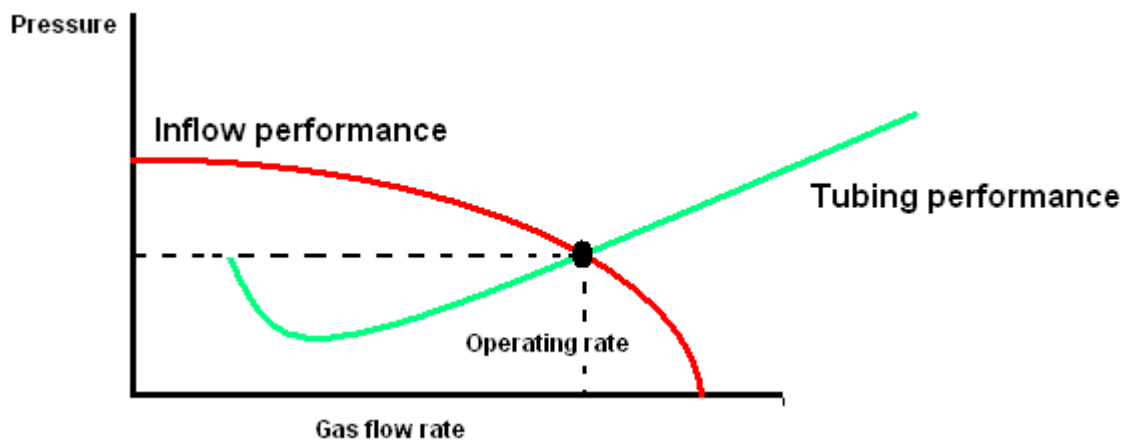


Figure 2.6: Illustration of Nodal analysis

3.0. MODELING FLUID FLOW

Jansen¹⁹ *et.al* developed a semi-analytical model that coupled a steady-state wellbore and reservoir flow for a conventional horizontal. The module was used to compute the inflow in extended stinger completions. With the aid of the module, the optimum configuration of stinger completion was obtained. The idea used by Jansen was of material assistance in development of the method used in this work to represent vertical well with a gas/liquid multiphase flow. The nature of the fluid flow being multiphase makes the solution to the problem solving to be more complex and involved than the single-phase flow problem solved by Jansen. In addition, for a vertical well friction is not the only important component to be calculated but more importantly is the hydrostatic component of the pressure gradient.

We start the modeling work by establishing the logical relationship between each wellbore segment. Thereafter the description of the fluid flows will follow.

3.1. Geometrical Description

Wellbore geometry can be modeled using principle of superposition. Superposition principle applies to any physical system that is linear. For example, beam deflection can be modeled by representing load as stimuli and beam as a spring. The use of superposition principle would enable easy prescription of boundary conditions on the wellbore whilst studying the effect of variation in geometry size. Wellbore is illustrated with figure 3.1 and figure 3.2 shows the decomposition of wellbore system into four subsystems namely:

- Casing section
- Annulus section
- Velocity string section
- Tubing string section

The boundary conditions will be prescribed at the node points. They are signified as z_1 , z_2 , z_3 and z_4 .

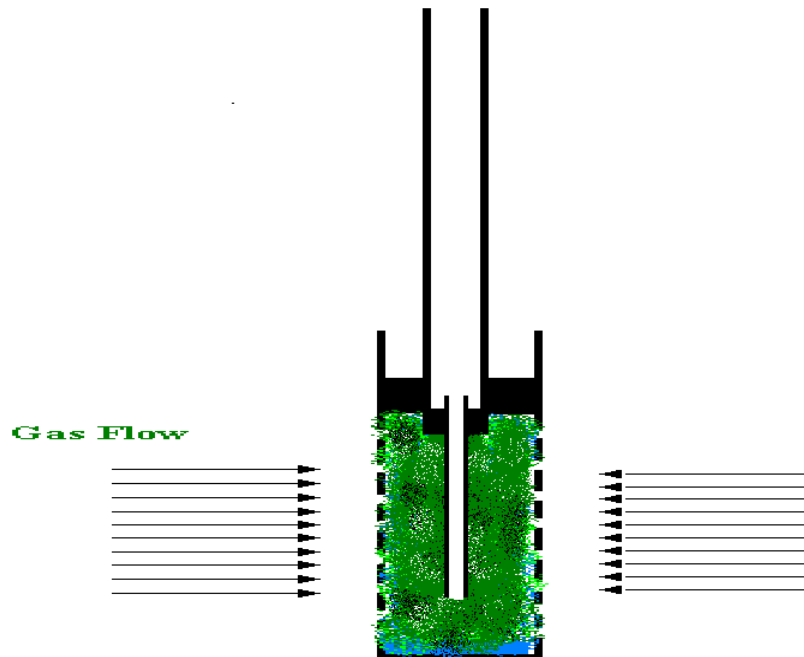


Figure 3.1: Illustrative representation of a Wellbore

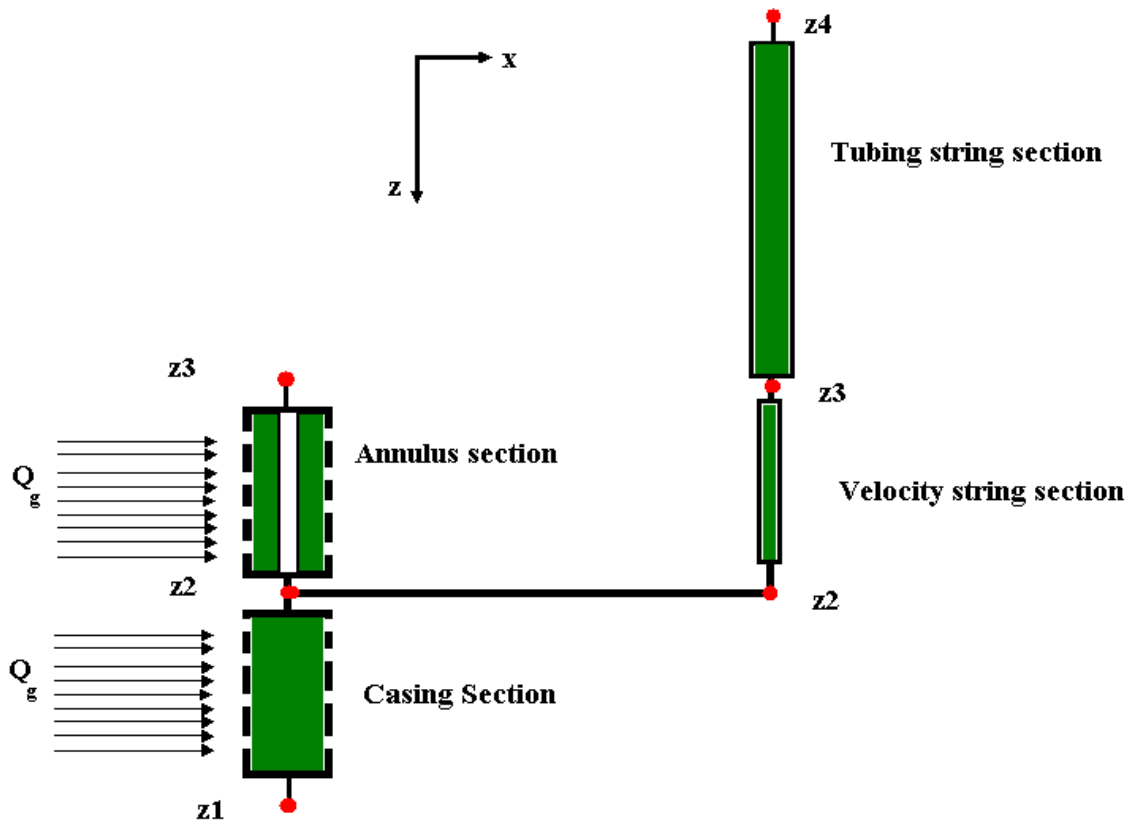


Figure 3.2: Schematic representation of the wellbore system

3.1.1. Geometric relation

By defining geometric relation between the different wellbore parts, the optimized variables can be clearly defined for use in the analysis.

The logical relationship that exists between the wellbore subsystems is obtained as the following:

Optimal Depth

Casing Shoe depth = z_1

Velocity string depth = z_2

Top of perforation depth = z_3

Total length of perforated interval $L_T = z_1 - z_3$

Casing length $L_{cas} = z_1 - z_2$

Annulus length $L_{ann} = z_2 - z_3$

Velocity string length $L_{vs} = z_2 - z_3$

Let define a dimensionless variable, which relates the ratio of velocity string length to total length of the perforated section as:

$$\beta = \frac{z_2 - z_3}{z_1 - z_3} \quad (3.1)$$

and $\beta = 0 \dots 1$ (range)

Hence total length of perforated interval can be re-expressed as

$$L_T = \beta L_{ann} + (1 - \beta) L_{cas} \quad (3.2)$$

To give some hindsight on the functional use of this dimensionless variable, the following will exemplify three different scenarios: when velocity string is set at the top of perforation, when velocity string is set at the half depth of perforated section and when velocity string is set at the bottom end of the casing shoe.

- Velocity string is set at the top of perforation

Using Eq.3.1 that means $z_2 = z_3$

$$\beta = \frac{z_3 - z_3}{z_1 - z_3} = 0$$

From Eq.3.2 the total length thus becomes

$$L_T = 0.L_{ann} + L_{cas} = L_{cas}$$

This implies the annulus section is eliminated in the analysis, remaining the casing and the tubing. Figure 3.3 shows that as the non-dimensional variable β changes from one to zero so does the depth of velocity string changes in the wellbore.

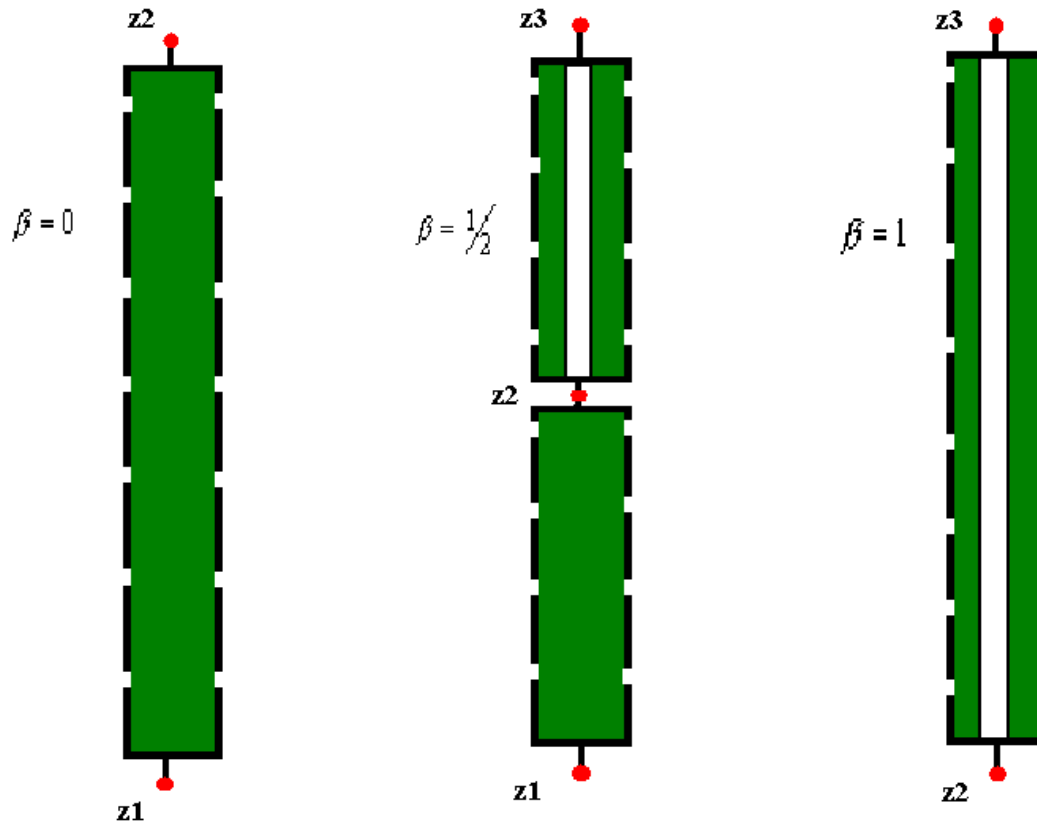


Figure 3.3: Velocity String variations

Another scenario is

- When velocity string is set at half depth of perforated section

From Eq. 3.1 $z_2 = \frac{1}{2}(z_1 + z_3)$

$$\beta = \frac{\left(\frac{z_1}{2} + \frac{z_3}{2}\right) - z_3}{z_1 - z_3} = \frac{\frac{1}{2}(z_1 - z_3)}{z_1 - z_3} = \frac{1}{2}$$

Thus the total length becomes

$$L_T = \frac{1}{2}L_{ann} + \frac{1}{2}L_{cas}$$

The final scenario is

- When velocity string is set at the bottom end of the casing shoe.

Thus $z_2 = z_1$, using Eq.3.1:

$$\beta = \frac{z_1 - z_3}{z_1 - z_3} = 1$$

Total length now becomes

$$L_T = L_{an} + 0 = L_{an}$$

Thus the range of the velocity string is within the interval of $L_{vs} : L_{ann} \leq z \leq L_{cas}$.

The use of the dimensionless length variable is illustrated in figure 3.4 as an example where possible curves for flow rates are plotted against non-dimensional length β . The corresponding location for maximum flowrate is considered as the optimum depth position, which could be represented as i.e. $\frac{1}{4}$, $\frac{1}{2}$ or $\frac{3}{4}$.

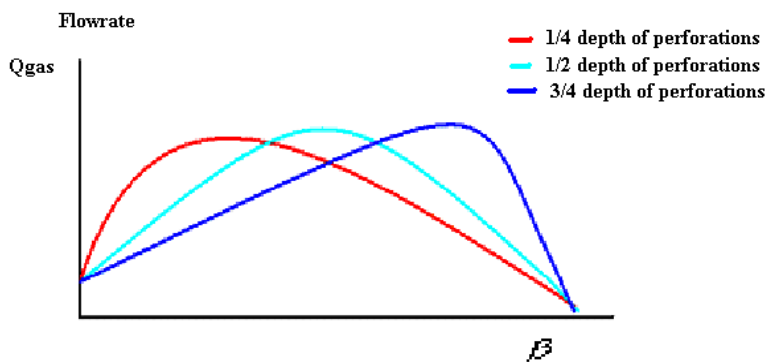


Figure 3.4: Example of Gas flowrate vs. non-dimensional length

Optimal Diameter

The relationships between the diameters are exemplified as:

$$\text{Casing Diameter} = d_c$$

$$\text{Velocity String OD} = d_{vso}$$

$$\text{Velocity String ID} = d_{vsi}$$

$$\text{Tubing ID} = d_{tb}$$

$$\text{Annulus Diameter (is calculated using Hydraulic diameter)} = d_c - d_{vso}$$

$$\text{Casing Area} = \frac{\pi d_c^2}{4}$$

$$\text{Velocity Inner Area} = \frac{\pi d_{vsi}^2}{4}$$

$$\text{Velocity String Outer Area} = \frac{\pi d_{vso}^2}{4}$$

$$\text{Tubing Area} = \frac{\pi d_{tb}^2}{4}$$

$$\text{Annulus Area} = \frac{\pi(d_c^2 - d_{vso}^2)}{4}$$

In optimizing the diameter size, it was decided to vary only the inner diameter of the velocity string d_{vsi} while its outer diameter remained fixed. Thus the range of d_{vsi} is within the interval: $0 \leq d_{vsi} \leq d_{vso}$ where Velocity String OD d_{vso} is prescribed.

3.2. Modeling of gas production

It is assumed that reservoir is homogeneous, steady state flow, radial and there is no cross flow between its formations. Principally we are interested in the estimation of the gas volumetric flowrate flowing from reservoir into the wellbore. Therefore, emphasis is not placed on the reservoir analysis.

It is assumed that the source of liquid in the flow stream is due to condensation of gasses to liquids in the wellbore as pressure and temperature decreasing. Liquids fallback and accumulate downhole. As a result of the accumulation of liquids downhole and rise in liquid column, the hydrostatic pressure increases and exerts pressure on the formation. Leaking off into formation is not considered in the analysis.

3.2.1. Inflow Modeling

Fluid flow into a wellbore is approximately proportional to the drawdown pressure, which is the difference between the higher-pressure reservoir and the lower sand face pressure. Using an empirical model developed by Rawlins& Schellardt for gas flow, gas inflow to the well is expressed as

$$Q_g(z) = C(p_r(z)^2 - p_{wf}(z)^2)^n \quad (3.3)$$

where

Q_g - Gas Flow rate [m³/s]

p_r - Reservoir pressure [Pa]

p_{wf} - Bottomhole pressure [Pa]

n is a value which varies between approximately 0.5 and 1.0. For a value of 0.5, turbulent losses are indicated; for a value of 1.0, no turbulence losses are indicated. The values of C and n are determined from well tests. At least two test rates are required because there are two unknowns, C and n , in the Eq.3.3; four test rates are recommended to minimize the effects of measurement error. Bottomhole pressure is the pressure value taken at the bottom end of production tubing downhole incase velocity string is installed; bottomhole pressure would be at the bottom end of velocity string.

Gas inflow is modeled by a single-phase flow. Liquid influx is incorporated in the fluid flow by making gas void in the Gray correlation equals zero at the casing shoe. A zero gas voids means the fluid is in liquid phase. Volumetric flowrate increases up through the perforations.

The reservoir pressure is assumed to be in static equilibrium. Thus, the reservoir pressure gradient along trajectories parallel to the wellbore is expressed as

$$\frac{dp_r}{dz} = \rho_g g \quad (3.4)$$

Here, the positive direction of z is in the vertically downward direction. The pressure gradient along the wellbore is described by a steady-state momentum balance and is expressed as

$$\frac{dp}{dz} = \rho_m g + \frac{v_m^2 \rho_m f}{2D_H} + \rho_m v_m \frac{dv_m}{dz} \quad (3.5)$$

D_H - Hydraulic diameter [m];
 f - Fanning friction factor [-];
 v_m - Mixture velocity [m/s];
 α_g - In situ gas fraction;
 g - Gravity

The mixture density depends on gas void and can be written as

$$\rho_m(z) = \rho_L(1 - \alpha_g(z)) + \rho_g(z)\alpha_g(z) \quad (3.6)$$

And mixture velocity is expressed as the sum of superficial gas velocity and superficial liquid velocity

$$v_m = v_{sg} + v_{sl} \quad (3.7)$$

Specific gas inflow into the well (flow rate per unit length) can be expressed as

$$q_{sg}(z) = C(p_r(z)^2 - p_{wf}(z)^2)^n \quad (3.8)$$

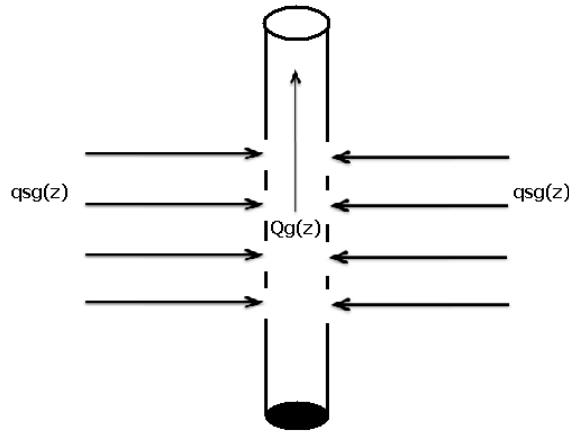


Figure 3.5: Schematic of vertical well, showing gas inflow

The cumulative gas inflow (Q_g) along the perforated sections is related to specific gas inflow by integrating the specific inflow into the well over the perforated sections

$$\frac{dQ_g(z)}{dz} = -q_{sg}(z) \quad (3.9)$$

The negative sign arises due to the convention that the coordinate z increases towards the far end of the well.

Gas flows continuously along the completed wellbore implies that the change in superficial velocity relates to specific gas inflow as

$$\frac{dv_{sg}}{dz} = -\frac{1}{\pi d^2/4} q_{sg}(z) \quad (3.10)$$

Continuous liquid influx under steady-state flow conditions implies that liquids that enter the wellbore are either produced, or seep back to the reservoir. We assumed that the flow is under steady-state conditions with no back-flow, hence the total liquid inflow rate equals liquid rate produced. Liquid superficial velocity in the wellbore then relates to gas superficial velocity and liquid fraction, R , associated with the gas

$$v_{sl} = v_{sg} R \quad (3.12)$$

Some authors treated gas density as a constant fluid property in their analysis²⁰. But a careful look at this fluid flow problem suggests that gas density is better determined in terms of pressure. Doing so would allow gas density to vary in relation to wellbore depth. Therefore the effect pressure change in relation to the phase density can be captured in the overall pressure drops. In addition, to fully capture the effect of interactions of all fluid properties and their flow conditions on the fluid flow performance, all the fluid properties are better define in their fundamental variables.

Gas density may be calculated by using engineering equation of state, which is expressed as

$$\rho_g = Ma \frac{P}{ZR_g T} \quad (3.13)$$

where

Ma - Apparent molecular weight [kg/Kmol]

P – Pressure [Pa]

Z – Compressibility factor [-]

R_g – Universal gas constant [8314 J/ (Kmol K)]

T – Temperature [K]

The units for all the variables have to be consistent. We have apparent molecular weight can be expressed as:

$$Ma = 28.96\gamma_g \quad (3.14)$$

γ_g - Specific gas density (air = 1)

3.2.2. Outflow Modeling

The intension here is to quantify the amount of gas volume transported to surface for a given time and production tubing size. When selecting velocity string ID size, there will be a balance between choosing large enough tubing diameter so that excessive friction will not occur and choosing small enough tubing diameter so that the velocity is high and thereby transporting liquid downhole to surface. The objective is to design a velocity string installation that meets these requirements over the entire flow conduit.

Mass flow rate through velocity and tubing string can be considered to be constant.

Therefore, mass flow rate gradient $\frac{d\rho_m Q_g}{dz}$, through the flow conduit can be expressed as:

$$\frac{d\rho_m Q_g}{dz} = 0 \quad (3.15)$$

Flow rate Q_g , is related to gas superficial velocity (v_{sg}) by

$$Q_g = v_{sg} (1 + R) \pi d^2 / 4 \quad (3.16)$$

d - Diameter [m]

$$R = \frac{V_{sl}}{V_{sg}} \quad [-]$$

Having all the essential equations that describe the transport phenomena in the wellbore, the next step is to assign these equations to their designated sections in the wellbore system. As it would soon be shown that many of these equations contain some complicated functions and the wellbore geometry is not a simple shape. Therefore solving the model equations analytically would be difficult. The best possible way to solve the system of non-linear equations is by *discretization* of the wellbore system. *Discretization* implies transforming a continuous model and equations into discrete counterparts.

3.3. Setting up Boundary conditions

Solving differential equations not only requires full specification of all essential variables but also its boundary conditions. Detail attention will be given to the *discretization* and the creation of the computational algorithm for the solution in chapter 4.

The focus of this part is to first state the boundary conditions that are readily known (*a priori*) around perforated section of the wellbore system.

3.3.1. Casing-Velocity String Annulus - Boundary conditions

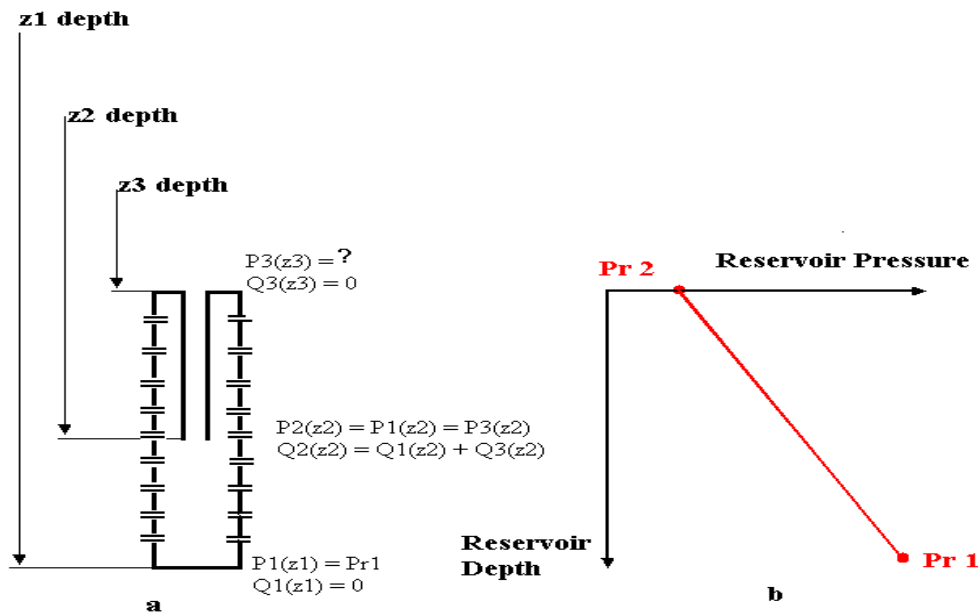


Figure 3.6: Perforated section of the Wellbore

Figure 3.6(a) presents the casing-velocity string annulus with casing shoe located at depth z_1 and the top of perforation at depth z_3 . Depth z_2 is the velocity string intake inlet.

It is assumed that the reservoir is in static equilibrium. Therefore its pressure gradient equation has only hydrostatic pressure, which increases with an increase in depth. The pressure values at casing shoe and top of perforations are represented by Pr_1 and Pr_2 respectively. These can be seen from figure 3.6 (b).

In differential equations, the order of the differentiation determines how many initial conditions or boundary values that are needed as *a priori*.

Pr_1 and Pr_2 are used as the initial pressure values in calculating flowing pressure from z_1 to z_3 (see figure 3.6 a).

At the bottom end of the wellbore, liquid accumulate and it is assumed that there is no backflow to the formation. Apparently, the end of the inflow interval corresponds to the

stagnant liquid level, which may be above the actual well bottom. In view of these reasoning, boundary condition at node 1 can be expressed as:

$$Q_g(z1) = 0 \quad (3.17)$$

Volumetric flow rate is zero is synonymous to superficial gas velocity being equals zero, therefore

$$v_{sg}(z1) = 0 \quad (3.18)$$

Boundary condition 3.18 implies that gas does not flow perpendicular to the casing shoe. The boundary conditions also suggest the existence of stagnant liquid at the base of the wellbore.

Bottomhole pressure at the casing shoe is equal to reservoir pressure

$$P_{wf}(z1) = Pr1 \quad (3.19)$$

At the top of the perforations, there is a packer that stops gas flowing through casing-tubing annulus as well as tubing-velocity string annulus. The following boundary conditions thus applied:

Packer stops gas flowing through implies that gas flow through the annulus is zero

$$Q_g(z3) = 0 \quad (3.20)$$

The constrain to the wellbore pressure is that pressure end value calculated from node 3 to 2 and node 1 to 2 must be equal

$$P_{1,2}(z2) = P_{3,2}(z2) \quad (3.21)$$

The pressure at node 3 which is at the top of perforation P3 (z1) (see figure 3.6) is a variable that depends on solution. It will be used to fix the condition (3.21).

3.3.2. Velocity String-Tubing Strings- Boundary conditions

The flow analysis in perforated wellbore section is different from velocity string because of the influx from reservoir through the perforations. Using the notation in figure 3.7, the traverse pressure as well as the other flow analysis can be carried out from bottom (z2) to top at the wellhead (z4) or from wellhead (z4) to bottom downhole (z2).

If the analysis would be from bottomhole to wellhead, the effort needs to be made such that wellhead pressure is fixed.

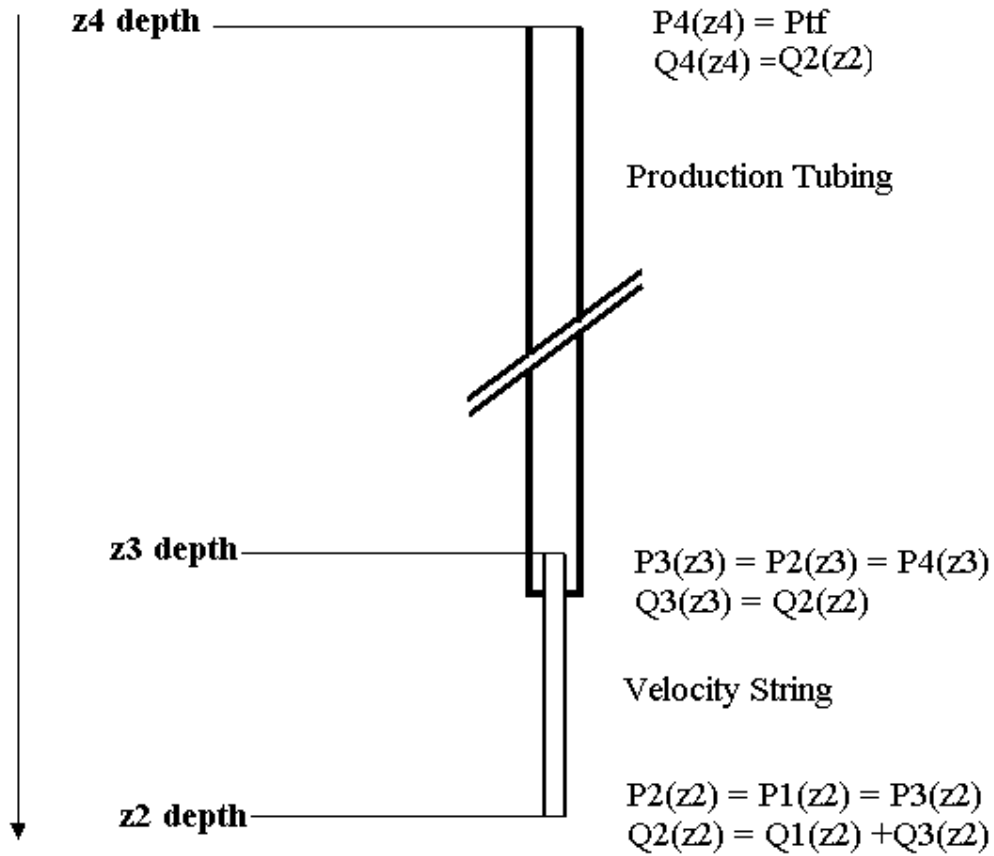


Figure 3.7: Velocity String- Production Tubing String completion

Pressure gradient through the velocity string is calculated by using pressure drop equation

$$\frac{dp}{dz} = \rho_m g + \frac{v_m^2 \rho_m f}{2D_e} + \rho_m v_m \frac{dv_m}{dz} \quad (3.22)$$

Since mass flow is not expected to increase or decrease while fluid is flowing through the velocity string, hence mass flow is conserved. Thus the wellbore model assumes two-phase homogeneous flow. That means mass conservation equations and the momentum equations under isothermal conditions can be applied. It is assumed that flow regime through the velocity string and production tubing is in annular mist flow; therefore conservation of mass flow through the stringer and production tubing strings can be expressed as

$$\dot{m} = \rho_m Q_g \quad (3.23)$$

\dot{m} - Mass flux [kg/s]

ρ_m - Mixture density [kg/m³]

Q_g - Volumetric flow rate [m³/s]

v_m Mixture velocity [m/s]

A- Flow conduit area [m²]

In differential form, conservation of mass flux through the tubing can be expressed as

$$\frac{d\dot{m}}{dz} = 0 \quad (3.24)$$

Substitution of equation (3.23) into (3.24) leads to

$$Q_g \frac{d\rho_m}{dz} + \rho_m \frac{dQ_g}{dz} = 0 \quad (3.25)$$

Now becomes

$$\frac{dQ_g}{dz} = -\left(\frac{Q_g}{\rho_m}\right) \frac{d\rho_m}{dz} \quad (3.26)$$

Or

$$\frac{dv_m}{dz} = -\left(\frac{v_m}{\rho_m}\right) \frac{d\rho_m}{dz} \quad (3.27)$$

Pressure at the top z_4 is the prescribed wellhead pressure P_{wf} . Thus

$$P(z_4) = P_{wf} \quad (3.38)$$

3.4. Estimation of pressure in the wellbore

Most of the pressure drop models developed in the oil and gas industry are models meant for estimating pressure drop in tubing string; little attention is paid to the development of pressure drop model for wellbore perforated section. This is largely due to the fact that the length of the perforated section is short when compared with the tubing string length. Factors such as perforation roughness, relatively big casing diameter size may cause an extra pressure drop. For example, perforation roughness can cause extra pressure drop due to boundary layer flow separation, recirculation and reattachment in and around a perforation in the casing string wall. Wrong estimation of wall roughness will be a potential source of error in pressure drop estimation. Gray correlation⁵ pressure model however takes into account this effect by allowing liquid film at the wall form a pseudo wall roughness thereby reduces friction factor. Introduction of pseudo wall roughness

reflects the observation that the frictional pressure drops observed in smooth laboratory piping exceeded the friction in corroded field piping. The assumption was that the liquid film at the wall reduced the friction and that this effect increased at higher gas velocities.

It has been noted that for very low velocities the pseudo roughness in Gray correlation could exceed the diameter in equations¹⁵. Practically this is of little relevance since at such low velocities the wells will be loaded with liquids, the flow regime will be intermittent or even bubble flow and the Gray correlation can not be considered valid any more.

There are indications that Gray correlation can be extended beyond its original bounds such as its limit with respect to size of tubing diameter²¹.

In chapter 2, it was explained that when gas velocity is below critical velocity, liquid droplet will fall back and accumulate to form liquid column. To allow for standing liquid column at the bottom well, Kutateladze number is introduced as a threshold that fence-off when liquid is lifted and when it falls back. Kutateladze number is expressed as

$$Ku = \left(\frac{\rho_g^{1/2}}{((\rho_l - \rho_g)g\sigma)^{1/4}} \right) v_{sg} \quad (3.29)$$

In a complete turbulent flow regime ($Re > 1635$), entrainment of liquid would happen³³ for Kutateladze number (Ku) greater than 3.2

$$Ku > 3.2 \quad (3.30)$$

At this critical value of Kutateladze number Ku , the flow regime changes from continuous to intermittent flow. This critical value of Kutateladze number also depends on deviation angle ϕ from the vertical. However, we shall restrict our analysis to a vertical well.

The following procedure will be used to calculate gas hold-up α_g in pressure gradient module. The procedure goes as follows:

if

$$Ku > 3.1 * (1 + 0.31 * \sin(2 * \phi))$$

$$A = 0.0814 \left(1 - 0.554 \ln \left(1 + \frac{730R}{R+1} \right) \right)$$

$$B = -2.2314 \left(Nv \left(1 + \frac{250}{Nd} \right) \right)^A$$

$$\alpha_g = \frac{1 - \exp^B}{R + 1}$$

else

$$\alpha_g = \frac{R + (-v_b / v_{sg})}{R + 1 + (v_b / v_{sg})}$$

With the bubble rise velocity v_b is calculated according to:

$$v_b = 0.345 \sqrt{Dg \frac{\rho_l - \rho_g}{\rho_l}}$$

end

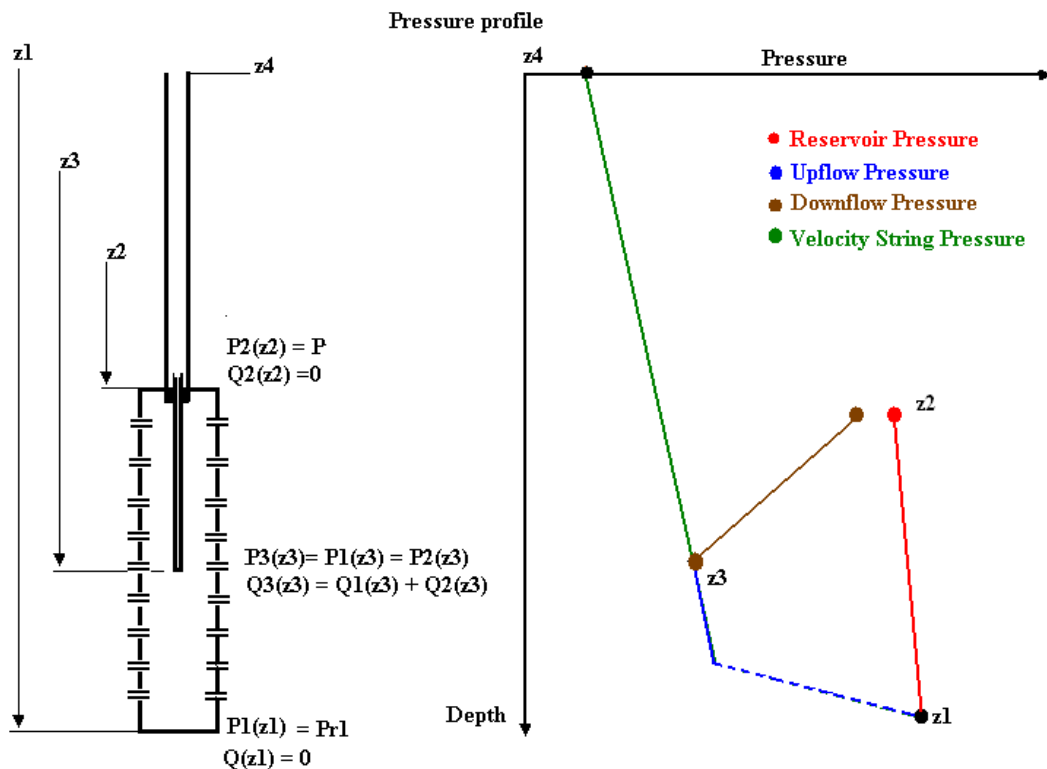


Figure 3.8: Illustrated Pressure profiles in the wellbore

In estimating pressure drop in the perforated section, there are two pressure gradient models required. As an illustration of how pressure profile in the integrated wellbore System might look like, figure 3.8 shows an illustrative pressure profile of the whole system couple with reservoir static pressure profile. The next section will discuss the treatment of pressure at the region where fluid flow downwardly before it enters through inlet of velocity string at $z3$.

3.4.1. The Down flow Pressure Gradient

Hydrostatic pressure is most often the major contributor to the total pressure gradient in a two-phase vertical flow. Hydrostatic pressure is directly proportional to the in-situ volume fraction phases. That is why it is very important to estimate the gas hold-up α_g accurately.

However, two-phase flow in the downward direction is not yet sufficiently understood to allow proper estimation of void fraction under various circumstances. Gas void fraction depends on in-situ velocity of gas phase. For up flow, buoyancy effect and the tendency of the gas bubbles to flow through the channel centre causes the in-situ gas velocity to be higher than the mixture velocity. For down flow, buoyancy opposes the flow of the gas phase. The cross sectional distribution of the gas phase in the channel may also be different from that in upflow²². Furthermore, the effect of buoyancy and bubble distribution across the channel depends on the existing flow pattern or flow regime.

In the course of this analysis, it is assumed that for downflow, both gas velocity and liquid velocity travel with the same speed, thus there is no slippage between the phase's velocities. This approach is referred to as homogeneous model approach. The pressure gradient equation for downflow can be written as

$$\frac{dp}{dz} = -\rho_n g + \frac{v_m^2 \rho_n f}{2D_e} + \rho_n v_m \frac{dv_m}{dz} \quad (3.31)$$

Where fluid density is expressed as

$$\rho_n = \lambda_g \rho_g + (1 - \lambda_g) \rho_l \quad (3.32)$$

ρ_n is a non-slip density. It is a kind density which would exist if both phases moved through the flow string at equal velocities. This homogeneous approach works well in a limited number of cases. Whalley (1987) states that this approach gives good result if the ratio of liquid and gas density is below 10 ($\rho_l / \rho_g < 10$) or if the total mass flux is greater than 2000 kg/ m²s ($Q_m > 2000$ kg/ m²s). Olieman³³ states that for oil/gas production this homogeneous flow model is suitable as a reference case especially in a high rate production.

The non-slip gas volume fraction λ_g is the ratio of superficial gas velocity to mixture velocity

$$\lambda_g = \frac{v_{sg}}{v_m} \quad (3.33)$$

And its corresponding liquid fraction is calculated accordingly as

$$\lambda_l = \frac{v_{sl}}{v_m} \quad (3.34)$$

Note that $\lambda_l + \lambda_g = 1$. (3.35)

Mixture velocity is summation of superficial gas velocity and superficial liquid velocity

$$v_m = v_{sg} + v_{sl} \quad (3.36)$$

Superficial liquid velocity is related to superficial gas velocity by this expression

$$v_{sl} = v_{sg} R \quad (3.37)$$

where

$$R = \frac{v_{sl}}{v_{sg}}$$

R is superficial Liquid/ gas ratio. Equation 3.35 can be re-expressed as

$$\lambda_g = \frac{1}{(1 + R)} \quad (3.38)$$

Gas volume fraction λ_g Eq. 3.38 is virtually constant value. Owing to slip effect accommodated by gas hold-up α_g in its formulation, gas hold-up will be smaller than the liquid volume fraction λ_g :

$$\alpha_g \leq \lambda_g \quad (3.39)$$

3.5. Model Equations

The following section will present all the equations related to each section of the wellbore in a compact form.

Once again the model equation as shown in figure 3.9 are presented as follows

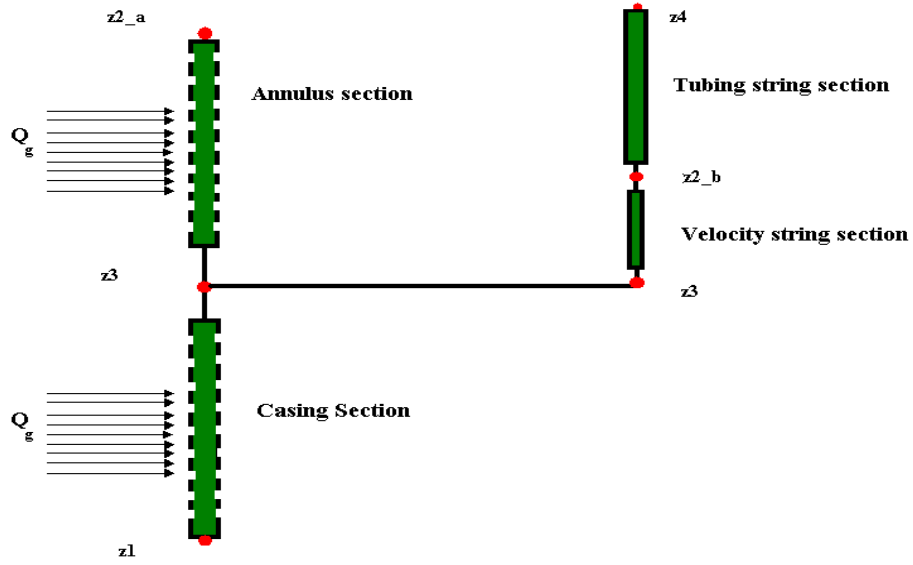


Figure 3.9: Wellbore representation

- For the casing section

$$\left\{ \begin{array}{l} \frac{dp_{wf}}{dz} = \rho_m g + \frac{f_w \rho_m v_m^2}{2d_c} \\ \frac{dv_{sg}}{dz} = -\frac{C(P_{res} - P_{wf}(z))^n}{\pi d_c^2 / 4} \\ \frac{dp_{res}}{dz} = \rho_g g \end{array} \right. \quad (3.40)$$

- For the Annulus section

$$\left\{ \begin{array}{l} \frac{dp_{res}}{dz} = \rho_g g \\ \frac{dp_{wf}}{dz} = -\rho_n g + \frac{f_p \rho_n v_m^2}{2(d_c - d_{vso})} \\ \frac{dv_{sg}}{dz} = \frac{C(P_{res} - P_{wf}(z))^n}{\pi (d_c^2 - d_{vso}^2) / 4} \end{array} \right. \quad (3.41)$$

- For the Velocity String section

$$\begin{cases} \frac{dp_{wf}}{dz} = \rho_m g + \frac{8Q_g^2 \rho_m f_{tp}}{\pi^2 d_{vs,i}^5} \\ \frac{d\rho_m Q_g}{dz} = 0 \end{cases} \quad (3.42)$$

- For production tubing string

$$\begin{cases} \frac{dp_{wf}}{dz} = \rho_m g + \frac{8Q_g^2 \rho_m f_{tp}}{\pi^2 d_t^5} \\ \frac{d\rho_m Q_g}{dz} = 0 \end{cases} \quad (3.43)$$

4.0. NUMERICAL ANALYSIS

A numerical method is more efficient to calculate the module equations proposed in chapter three than analytical methods. The basic principle behind this coupled model is the pressure continuity and mass balance at the sand face. In an ideal case, integration could have been performed at once, such that pressure continuity along the wellbore is ensured. But it is apparent that there is a piecewise discontinuity of pressure profile at the inlet of the velocity string. Therefore the numerical integration is carried out at each segment of the wellbore. The fluid flow equation is solved using an explicit Runge-Kutta numerical scheme. The fluid flow path can be approximated in 1D without loss of detail.

4.1. Numerical scheme representation

The following analysis will show how the model equations in chapter 3 can be solved numerically. The sequence used here is also implemented for computational algorithm. We decided to include temperature gradient into the module equations. It is assumed that the well formation temperature is isothermal with an average change of 0.02 per unit length.

For the Casing section

$$X1 = p_{wf}, X2 = v_{sg}, X3 = p_{res}, X4 = T,$$

$$\frac{d}{dz} \begin{bmatrix} X1 \\ X2 \\ X3 \\ X4 \\ X5 \end{bmatrix} = \begin{bmatrix} \rho_m g + \frac{f_w \rho_m v_m^2}{2d_c} \\ -X5 \\ \rho_g g \\ 0.02 \end{bmatrix} \quad (4.1)$$

Note $T = \text{Temperature}$

For the annulus section

$$X1 = p_{wf}, X2 = v_{sg}, X3 = p_{res}, X4 = T$$

$$\frac{d}{dz} \begin{bmatrix} X1 \\ X2 \\ X3 \\ X4 \end{bmatrix} = \begin{bmatrix} -X1 \\ X2 \\ \rho_g g \\ 0.02 \end{bmatrix} \quad (4.2)$$

For the Velocity String section

$$X1 = p_{wf}, X2 = Q, X3 = T$$

$$\frac{d}{dz} \begin{bmatrix} X1 \\ X2 \\ X3 \end{bmatrix} = \begin{bmatrix} \rho_m g + \frac{8X2^2 \rho_m f_{ip}}{\pi^2 d_{vs,i}^5} \\ 0 \\ 0.02 \end{bmatrix} \quad (4.3)$$

For the production tubing string

$$X1 = p_{wf}, X2 = Q, X3 = T$$

$$\frac{d}{dz} \begin{bmatrix} X1 \\ X2 \\ X3 \end{bmatrix} = \begin{bmatrix} \rho_m g + \frac{8X2^2 \rho_m f_{ip}}{\pi^2 d_t^5} \\ 0 \\ 0.02 \end{bmatrix} \quad (4.4)$$

4.2. Flow chart for computational algorithm of fluid flow model

As an illustration of how computation progresses along the grids, figure 4.1 shows the numerical solution of the system of equation (4.1-4.4). The computation starts by solving all variables at node1 (casing shoe) to node 3 (velocity string inlet) and a parallel computation from node 2 (sealed parker for casing –tubing annulus) to node 3 again. Another computation starts from node 4 -wellhead to node 3 (the inlet of the velocity string).

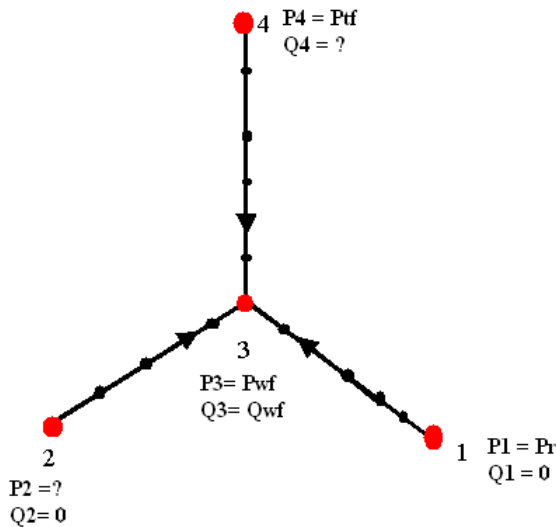


Figure 4.1: Grid representation of the wellbore

The computation of each node - 1, 2 and 3 can be performed with appropriate boundary conditions. The only difficulty here is that the boundary value problem is made up of three boundary conditions instead of the two boundary conditions commonly encounter in differential equations. *The Math Works* has developed method for transforming multipoint boundary value problem into a two-boundary value problem.

Alternatively, the computation can be done sequentially. The computation starts from wellbore casing – node 1 to node 3(velocity string inlet). The values for pressure and gas velocity are stored. The next computation of pressure and gas velocity is carried out from node 2 to node 3. A node having two pressure values at the same level suppose to be equal. Therefore, the two pressure values at the node 3 suppose to have the same value. However, it is most likely this will not happen. The pressure profiles plot might look like the one shown in figure 4.2. The figure 4.2 illustrates an unmatched pressure profiles. To fix the problem, the pressure value at node 2 has to be change until the pressure end value at node 3 match together. Every time we set a new depth for z_3 , only P2 needs to be changed at node 3 . Figure 4.3 presents flowchart for eventual creation of computational algorithm.

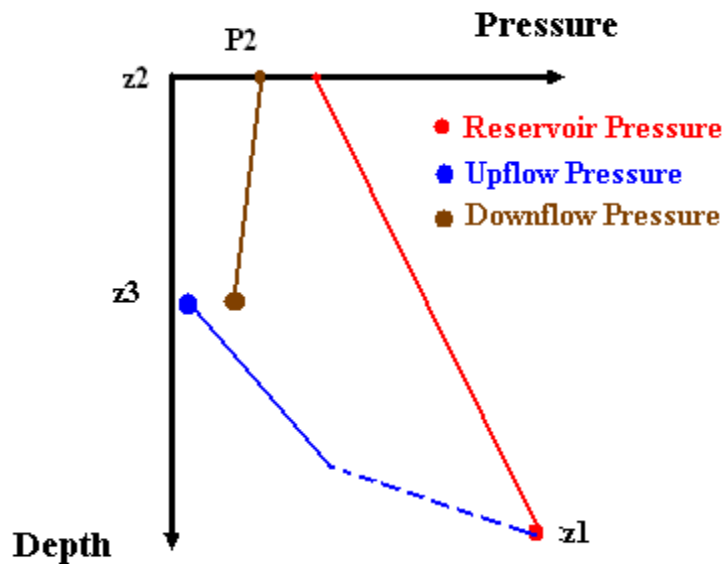


Figure 4.2: An illustrated example of unmatched pressure profiles

Lea, Nickens and Wells explain in their book, “Gas Well Deliquification-Solution to Gas Well Liquid Loading Problems” page 39 that if the critical velocity is exceeded at the bottom end of the velocity string, then it will be exceeded everywhere in the tubing string. What this implies is that the gas velocity obtained at the inlet of velocity string is directly proportional to what would be obtainable at the wellhead.

In spite of simplicity of the model presented here, the module computation can get quite involved. The primary source of complications is when input data are not in appropriate order. The computation becomes *stiff*; as a result the computation iteration will not converge.

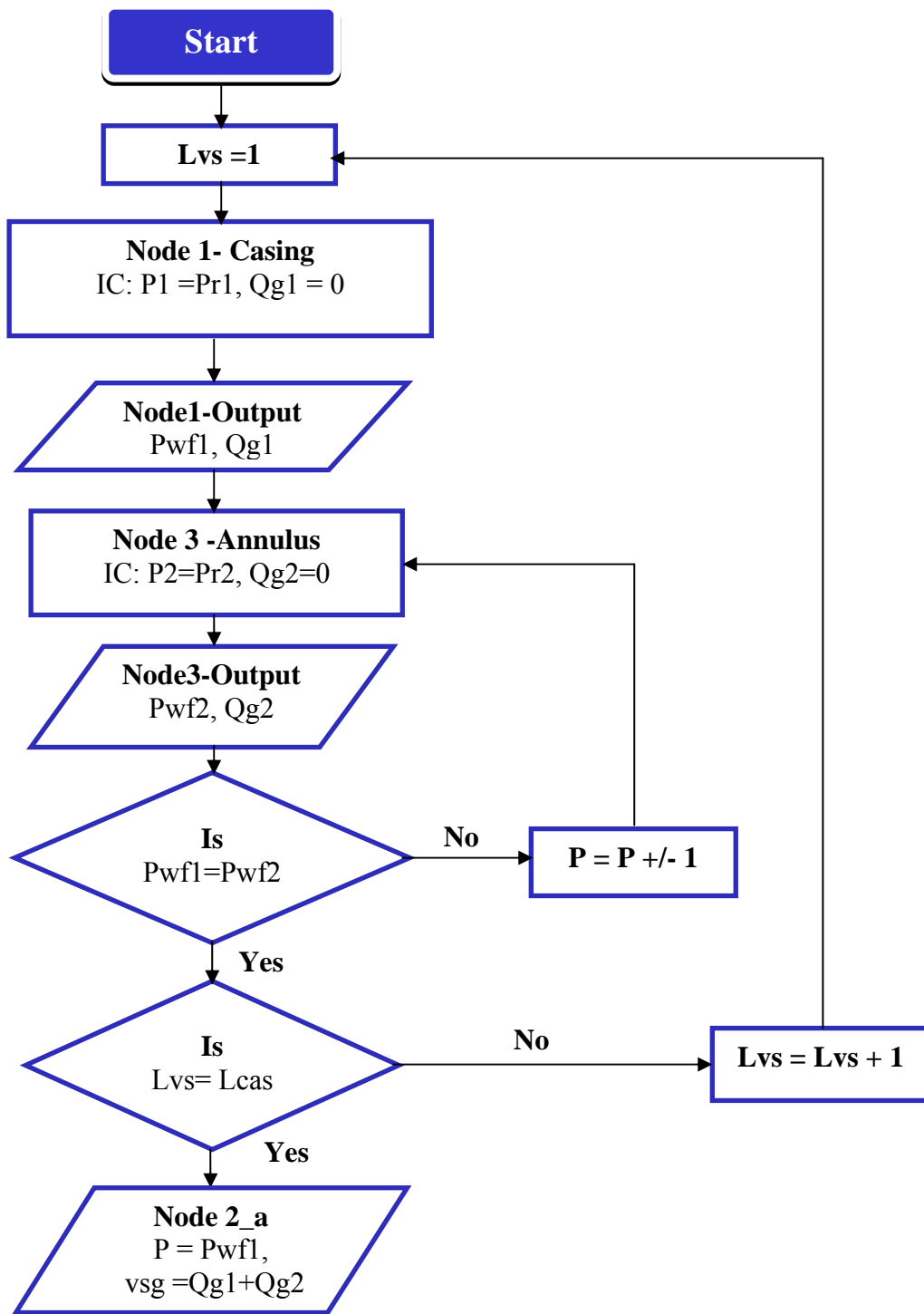


Figure 4.3: Flowchart for computation algorithm

5.0. RESULTS & DISCUSSION

A demonstration of a problem scenario is given in this chapter. Through the problem example, the model equations developed earlier is used to analyze the optimization parameters for a velocity string.

5.1. Example Calculations

A gas well has the following data:

Well depth = 3000m

Top of perforation depth = 2900m

Well head pressure = 114bar

Reservoir Pressure= 150 bar

Reservoir Temperature = 350 K

Reservoir height = 100m

C (coeficiente in Eq.1) = $2.2981e-011 \text{ m}^3/\text{s}/\text{Pa}^{2n}$

$n = 0.6$

LGR=R = 0.00075

Velocity string ID= 0.02m / 0.04m/ 0.06m OD= 0.085m

Tubing ID = 0.08m Tubing OD= 0.085m

Casing ID= 0.15m

Liquid density = $850 \text{ kg}/\text{m}^3$

Liquid viscosity= 0.000013 Pa.s

Gas viscosity = 0.0005 Pa.s

Surface tension = 0.0199 N/m

Boundary Conditions Used for Simulation:

Pressure at the casing shoe = 150 bar

Superficial Gas Velocity at the casing shoe = 0 m/s

Superficial gas Velocity at the top of perforation = 0 m/s

All solutions are calculated in reservoir (*in-situ*) condition. Thus fluid properties are not calculated at standard condition.

5.2. Velocity string Optimal Depth

We first considered situation when there is no velocity string installed in the wellbore. Figure 5.1 shows the wellbore pressure traverse. It can be seen that at the depth close to 3000m the pressure profile has high-pressure gradient. The high gradient is due to the liquid accumulated downhole.

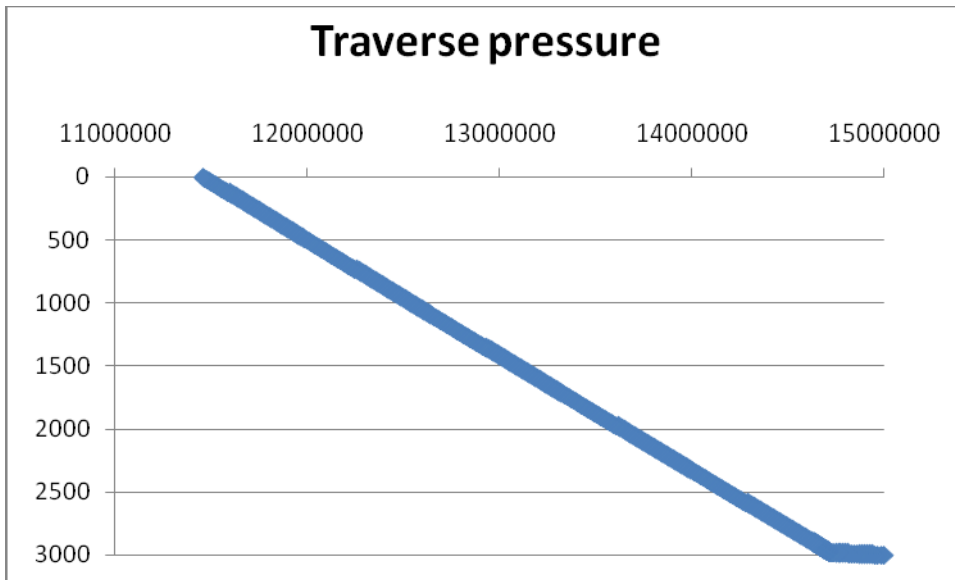


Figure 5.1: Pressure Traverse

Figure 5.2 shows pressure profiles in the perforated wellbore section. It can be seen that transition from intermittent flow (bubble - slug flow) regime occurred at 2978m depth.

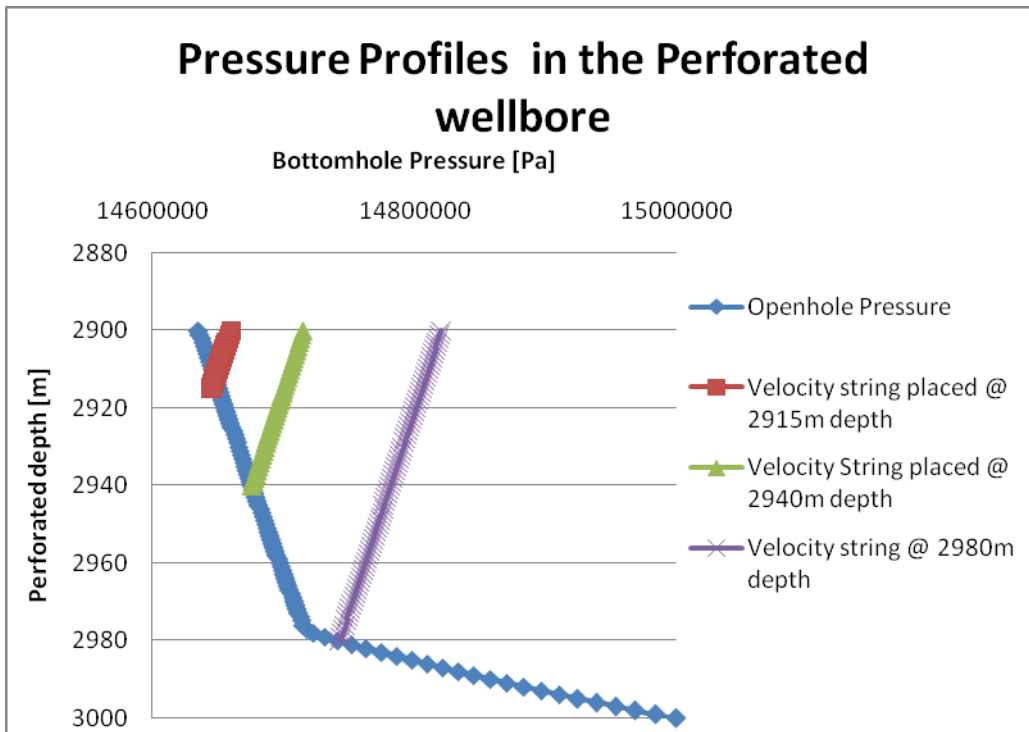


Figure 5.2: Wellbore pressure along the perforated section

Bottomhole pressure for different velocity string setting depths can be determined from figure 5.2. The bottomhole pressure values for different velocity setting depths are

determined from the intersection of open hole pressure profile and the velocity string pressure profiles. At these intersection points, there we read the corresponding gas velocity of each setting depth.

The resulting velocities for each setting depth are plotted over the length of perforation portion of the wellbore.

Figure 5.3 shows the plot curve of the calculated mixture velocity at various velocity strings setting depth which ranges from 2900m to 3000m. At 2900m there is no string installed and there the mixture velocity reads 6.5m/s. When the stringer is lowered down to the depth of 2960m, it can be seen from figure 5.3 that the mixture velocity attains the value of 7.5m/s. At that setting depth the optimum velocity is attained. When the setting depth is further increased to 2900m depth, there the mixture velocity becomes zero, meaning that there is no more fluid flowing. At that depth, the stringer has been brought in contact with the standing liquid column downhole. Even before the stringer got in contact with the liquid column at 2900m depth, the rate at which mixture gas velocity declines from 2975m depth to 2900m depth is so rapid. This implies that velocity string performance is susceptible to liquid. Therefore for an effective use of velocity string, it has to be placed away from loaded region. By placing the stringer at the optimum depth of 2960m the gas mixture velocity is increased by 15%.

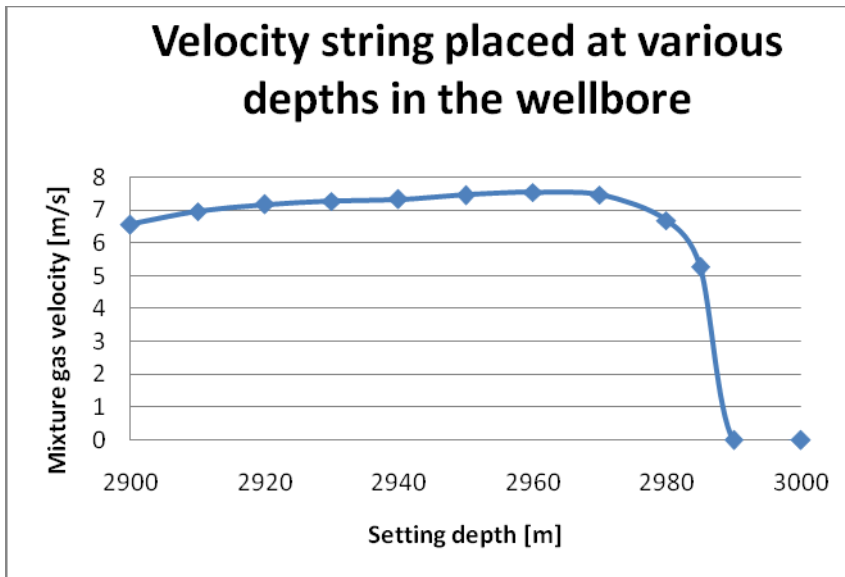


Figure 5.3: Flow rate vs. Setting depth

5.3. Selection of Optimum Diameter Size

The optimum diameter size is determined by plotting the reservoir inflow performance curve (IPR) and tubing performance curve (TPC) for various tubing diameter size.

Consider the following candidate ID: 0.02m, 0.04m, 0.06m and 0.08m. Figure 5.4 shows the nodal analysis of the given diameter sizes.

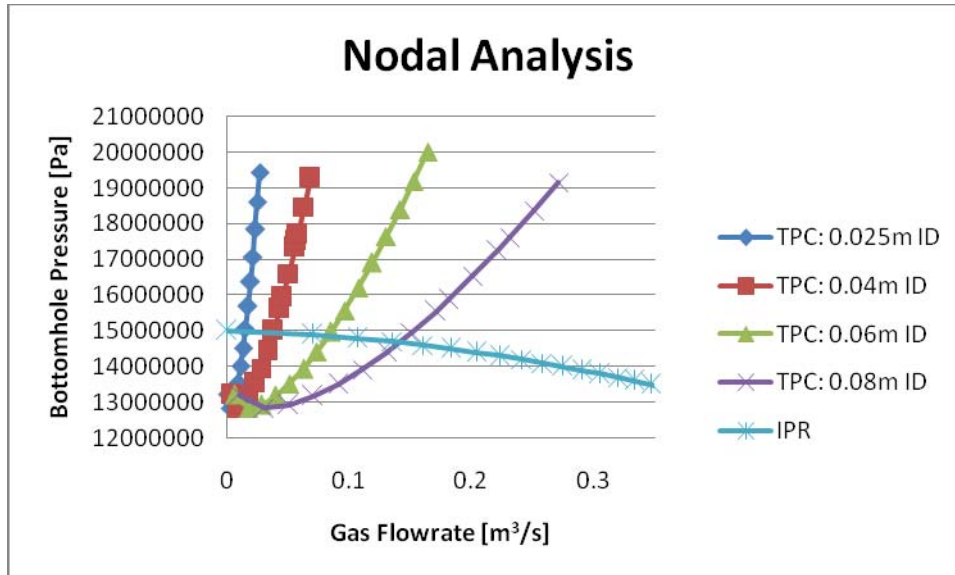


Figure 5.4: Nodal Analysis

To have the proper view of the whole data, Table 5.1 presents the data for the whole selected candidates

Table 5.1: Presentation of the Nodal results for different diameter sizes

Velocity String ID (m)	0.02	0.04	0.06	0.08
Nodal Solution pressure (10^7 Pa)	1.5	1.499	1.47	1.46
Nodal solution rate (m^3/s)	0.016	0.037	0.07	0.135
Critical rate for Nodal solution pressure (m^3/s)	0.014	0.016	0.03	0.04

By close examination, the tubing size 0.06m and 0.08m deliver more gas than the other two – 0.02m and 0.04m tubing diameter. But if one would consider longevity as criteria, it is better to choose 0.06m tubing diameter size because it will still be more suitable when reservoir pressure decline even further.

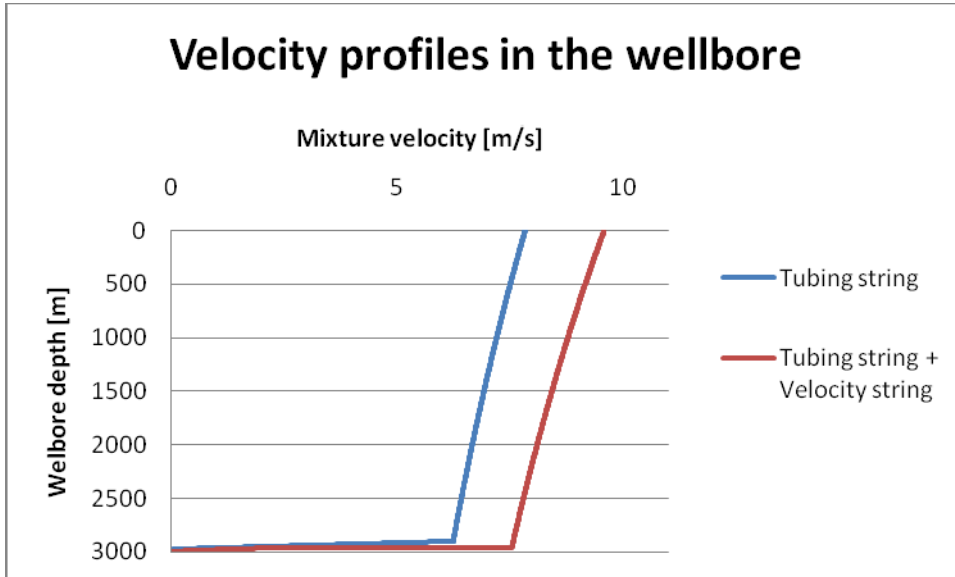


Figure 5.5: Velocity profiles along the wellbore

Figure 5.5 shows two velocity profiles. One is completed with velocity string and the other is not. When the well is completed with velocity string, the mixture velocity obtained at the wellhead is 9.59m/s. On the other hand when the well is not installed with velocity string the resulting velocity at the wellhead is 7.84%. Hence by installing velocity string into this particular liquid loaded well will increase gas velocity by 26%. The figure 5.5 also reveals that the gas velocity had to cross the threshold of 6 m/s before it starts rising up. Prior to the attainment of this velocity (6.5m/s), the fluid flow was in an intermittent flow regime. After the increase in gas mixture velocity, the flow transit from bubble – slug flow regime to annular mist flow. Through out the production tubing string up to the surface the flow regime remains in the annular mist flow.

6.0. CONCLUSION AND RECONMENDATIONS

A procedure for the design optimization of a velocity string used for combating liquid loading problem has been developed. The proposed fluid flow model which couples separate inflow from reservoir to an outflow performance with Gray correlations, can be used to optimize velocity string's length and diameter. The proposed model allows for existence of stagnant liquid column downhole the wellbore. In the model simulation, the depth of a velocity string can be varied and its corresponding flowrate can be calculated at each depth location.

A flowchart for computational algorithm has been proposed which is meant to aid implementation of the proposed module on a computer devise.

The model created has been used to determine an optimal position depth of a velocity string in the gas wells that suffer from liquid loading problem. The developed fluid flow model was implemented on a computer devise, it was shown that an optimal placement position is close to the depth at which transition between intermittent flow and annular mist flow occurred. It is has also be shown that effectiveness of velocity string is susceptible to liquid holdup in the well. Velocity string should better place clear away from bubbly and slug flow regime. It is remarkable to know that friction is the primary factors that affect the optimization.

It has also been established that construction of tubing performance curve can be used to select best candidate for tubing size diameter (ID). A demonstration of example problem reveals how design optimization can be done in selecting best candidate for velocity string diameter. A routine calculation has to be performed before a selection of an appropriate tubing size. The well data couples with history and forecast of the well are also essential to know when making selection.

The model work can be further upgraded to include cross-flow in the production zones, transient analysis module to predict volume of liquid that can be removed with the used of a given diameter before re-completion of the well. The approach used to calculate liquid hold-up for downflow pressure module in the analysis is homogeneous module approach. This approach may under-predict pressure value and as a consequent, it might over/underestimates flow rate. It is therefore recommended to subject the accuracy of the homogeneous module to further investigation.

REFERENCES

- [1] Duggan, J.O., "Estimating Flow Rates Required to Keep Gas Wells Unloaded", *J. of Pet. Tech.*, December 1961.
- [2] Turner, R.G., Hubbard, M.G., and Dukler, A.E., "Analysis and Prediction of Minimum Flow rate for the Continuous Removal of Liquids from Gas Wells", *J. of Pet. Tech.*, November 1969 1475-82; *Trans.*, AIME, 246.
- [3] Coleman, S. B., Clay, H. B., McCurdy, D. G., and Norris, H. L., III, "A New Look at Predicting Gas-Well Load Up," *Journal of Petroleum Technology*, March 1991, pp. 329-333.
- [4] Kumar, N., "Improvements for Flow Correlations for Gas Wells Experiencing Liquid Loading", SPE paper 92049, *Journal of Petroleum Technology*, April 2005.
- [5] Gray, H.E.: "Flowing Pressure Calculations for Gas/Condensate Wells", EPR Report 855, Shell Oil Corporation, 1955.
- [6] Cullender, M.H. and Smith, R.V.: "Practical Solution of Gas-Flow Equations for Wells and Pipelines, *Trans. AIME*, 1956, p281-287.
- [7] Poettman F.H. and Carpenter, P.G.: "The Multiphase Flow of Gas, Oil and Water Through Vertical Flow Strings with Application to the Design of Gas Lift Installations", *Drilling Production Practices*, API (1952), p257.
- [8] Bexendell, P.B. and Thomas, R.: "Calculation of Pressure Gradients in High-Rate Flowing wells", *Journal of Petroleum Technology* (October 1961) p1023.
- [9] Francher, G.H. & Brown, K.E.: "Prediction of Pressure Gradients for Multiphase Flow in Tubing", *Trans AIME* 140, 1963.
- [10] Duns, H., Jr. And Ros, N.C.J.: "Vertical Flow of Gas and Liquid Mixtures in Wells", *Proc. Sixth World Pet. Congress, Frankfurt* (June 19-26, 1963) Section II, Paper 22-PD6.
- [11] Orkiszewski, J.: "Predicting Two Phase Pressure Drops in Vertical Pipes", *J. Pet. Tech.* (June, 1967) p 829-838.
- [12] Beggs, H.D. and Brill, J.P.: "A study of Two-Phase Flow in Inclined Pipes", *J. Pet. Tech.* (May, 1973) p 607-617.
- [13] Dukler, A.E.: "Gas-Liquid Flow in Pipelines, I. Research Results", AGA-API Project Nx-28 (May 1969).
- [14] Brill, J.P., and Mukherjee H.: "Multiphase flow in Wells", Henry L. Doherty Memorial Funds of AIME, SPE Inc, Richardson, Texas, 1999.
- [15] Aziz, K., Govier, G.W. and Fogarasi, M.: "Pressure drop in wells Producing Oil and Gas", *Journal of Canadian Petroleum Technology*, (July-Sept. 1972) p 38-48.
- [15] Oudeman, P., "On the Flow Performance of Velocity Strings to Unload Wet Gas wells", SPE paper 104605, *Journal of Petroleum Technology*, March 2007.
- [16] Hassan, A.R., Kabir, C.S., and Rahman, R.: "Predicting Liquid Gradient in Pumping-Well Annulus," SPE (Feb. 1998) 113-20.
- [17] Wallis, G.B., "One dimensional two-phase flow", McGraw-Hill Book Company, 1969.
- [18] Oudeman, P., "Further Improvements of Gray Correlations for pressure drop over wet Gas Wells on the Basis of the vertical Flow Tests in NAM Well Amsweer-1", Group Research Report RKGR.90.010 NAM/Shell Expro/BEB Project on Liquid Loaded Gas Wells, May 1990.

- [19] J.D. Jansen: “Numerical modeling of flow in extended stringer completions”, Research Report for Shell International E&P, TU Delft (2000).
- [20] Asheim, H. & Oudeman, P.: “Liquid Loading along the Completed Section of Horizontal and Inclined Wells may govern Inflow Performance” SPE 36861 Paper, October 1996.
- [21] Kabir, C.S., “Simplified Wellbore-Flow Modeling in Gas/Condensate Systems” SPE 89754 Paper, June 2005.
- [22] Hassan, A.R.,” A Basic approach to Wellbore Two-Phase Flow Modeling” SPE 109868 Paper, November 2007.
- [23] Oudeman, P.,” Modeling to Understand Wet Gas Well Behavior Studying Wet Gas Wells with WePS”, Shell Research Report EP 2002-5302, July 2002.
- [24] Chiu. Ikoku: “Natural Gas Production Engineering”, John Wiley & Sons, (1984), New York, NY.
- [25] Brill, James P., Beggs, Dale H.: “Two –Phase flow in pipes”, Notes, April 1978
- [26] Lea J., Nickens, H., Wells, M.: “Gas Well Deliquification-Solution to Gas Well Liquid Loading Problems”, Elsevier, 2003 ,electronic ISBN: 978-0-0805-7798-5
- [27] Brennen, C.E.: “Fundamentals of Multiphase Flow”, Cambridge University Press (2005), ISBN-13 978-0-521-84804-6.
- [28] Corradini, Michael, L.: “Fundamentals of Multiphase flow”, <http://wins.engr.wisc.edu/teaching/mpfBook/>, last modified Monday August 4 1997.
- [29] Lyons, William C.; Plisga, Gary J. Standard Handbook of Petroleum & Natural Gas Engineering (2nd Edition). Elsevier. Online version available at: <http://www.knovel.com/knovel2/Toc.jsp? Book ID=1233&VerticalID=0>.
- [30] Frydenlund H., Vebeek P.H.J., Affeld, C.J.: “Liquid Unloading of Gas Wells- Intermittent Production by Downhole Separation and Gravity Drainage”, Shell Report, EP 2003-5307, September 2003, page 3.
- [31] Van Oosterhout, J.J.M. (1961), Vertical Gas Liquid flow as Encountered in oil Wells, Part VII, K/S EP Lab., Research Report R 1068, December 1961.
- [32] Rene V.A. Oliemans, “Multiphase flow Technology for production and transport of oil and gas” Extract of Lecture notes of TN378 presented to participant of learning centre of Royal Dutch Shell , May 2000, page 99.
- [33] Rene V.A. Oliemans, “Multiphase flow Technology for production and transport of oil and gas” Extract of Lecture notes of TN378 presented to participant of learning centre of Royal Dutch Shell , May 2000, page 55.

NOMENCLATURE

- A - Cross-sectional area of conduit [m^2]
 α_g - In situ gas fraction (gas hold-up) [-]
 β - Non-dimensional constant for length [-]
 C - Coefficient for productivity [$\text{m}^3/\text{s}/\text{Pa}^{2n}$]
 C_d - Drag coefficient [-], recommended a value 0.44.
 d_p - Liquid droplet diameter [m]
 D_H - Hydraulic diameter [m]
 d_c - Wellbore casing diameter [m]
 d_{vso} - Velocity String outside diameter [m]
 d_{vsi} - Velocity String inside diameter [m]
 d_{tb} - Tubing inside diameter [m]
 ε - Wall roughness [m]
 f - Friction factor [-]
 g - Gravitational acceleration [m/s^2]
ID – inside diameter [m]
OD- Outside diameter [m]
Ku- Kutateladze number [-]
 L_T - Total perforated length [m]
 L_{cas} - Wellbore casing length
 L_{an} - Tubing –casing annulus length [m]
 L_{vs} - velocity string length [m]
LGR – Liquid gas ratio [-]
Ma- Apparent molecular weight [kg/Kmol]
 n - exponent for Rawlins& Schellardt equation [-]
 N_{we} - Weber number [-]
 σ - Interfacial (surface) tension between liquid and gas
 σ_l - Gas-liquid interfacial tension [dyne/cm]
 $\sigma_{m,w,c}$ - Mixture interfacial tension [dyne/cm]
 ρ - Densities of gas and liquid at wellhead conditions [kg/m^3]
 $\rho_{g,l}$ -Gas, Liquid densities [kg/m^3]
 ρ_m - Mixture density [kg/m^3]
 ϕ - Deviation angle from vertical [rad]
 λ_g - gas volume fraction [-]
 p_r - Reservoir pressure [Pa]
 p_{wf} - Bottomhole pressure [Pa]

P_{wf} - Wellhead pressure [Pa]

p_d - Dew point pressure [psi]

p - Pressure at depth of interest [Pa]

$\rho_{g,l}$ - Gas, Liquid densities [kg/m³]

μ_{av} - Average viscosity of the liquid and gas phase [Pa s].

Q_g - Gas Flow rate [m³/s]

Q_{gm} - The minimum required gas flow for liquid removal [MMscf/day]

r - pseudo wall roughness [ft]

r_g - absolute wall roughness for dry gas flow [ft]

R_g - Universal gas constant [8314 J/ (Kmol K)]

R - superficial liquid/gas ratio (in situ) [-]

T - Temperature (K)

v_g - *In situ* gas velocity [m/s]

$V_{so,w,g}$ - Oil, Water, Gas superficial velocity

v_m - Mixture velocity [m/s]

v_c - Critical velocity [m/s]

v_b - bubble rise velocity [m/s]

γ_g - Specific gravity [-]

z - depth [m]

Z - Gas compressibility factor [-]

APPENDIX B: Computer code

This code is compiled by *Matlab* compiler. The main program is called *solution.m*, the function that does computation on each section segment in the wellbore are designated by their respective names i.e. *wellbore.m* does computation on casing section, *annulus.m* does computation on the annulus section similarly *velocitystring.m* and *tubing-string.m* perform computation on velocity string and tubing strings respectively.

```
%%%%%%%%%%
clc;
clear;
close all;

global dvsi dvso dci dh g Ah Ma Rg k h re S D So Z dt At
global R miug Ac rg miul n c C sigma rho1 theta gammag Twf

top_of_perforation=2900;% [m]
bottom_of_perforation=3000;% [m]
Velocity_String_Depth=2950;% [m]
Reservoir_pressure=1.50e+007;% [Pa]
vsg_0= 1.0e-00016;% [m/s] it is apperently equals to zero
Reservoir_temperature=350;% [K]

%-----Algorithm
%-----reservoir pressure is calculated independently--- its
values
%are used as an input for subsequent computation

zspan=[bottom_of_perforation :-1: top_of_perforation];%---- perforated
interval
P_in=[Reservoir_pressure;%---Initial Condition: reservoir pressure at
casing shoe
350];%----reservoir Temperature
[z,x] =ode45('P_reservoir',zspan,P_in);%-----calaculation carried out

%%----- Algorithm for wellbore section
%%(1) Node 1 to Node 3a
zwspan=[bottom_of_perforation :-1: Velocity_String_Depth];

%%----- Initial conditions-----
xw0=[Reservoir_pressure-0.000001;
vsg_0
Reservoir_pressure
Reservoir_temperature]

[zw,xw] =ode45('wellbore',zwspan,xw0);

%-----Input Data%-----

n= 0.6; %% [-] n=0.5- 1; meaning from turbulent flow to laminar flow
% c= 0.002 ;%% [Mscf/D/psi^2n]
```

```

C= 2.2981e-011;% c*0.32774128472/(6894.757293178^(2*n));%% converted to
SI unit
g=9.81;
sigma=0.0199; %[N/m] surface tension

Z=0.981;% [-] compressibility

rho_l= 850; % [kg/m^3] water density
mu_g=0.000013; %[Pa.s] gas viscosity
mu_l=0.0005; % [Pa.s]; liquid viscosity
gamma_g=0.650;
Ma= gamma_g*28.96; % [kg]molar mass
Rg = 8314; % [-] gas Constant
dci=0.15; % [m] inner casing diameter
pipe_thickness=0.02; %%[m]
dvs_i= 0.06 ; % inner velocity string diameter [m]
dvs_o= 0.085; % outer velocity string diameter [m]
dh=dci-dvs_o; %hydraulic diameter [m]
dt= 0.080; %% production tubing diameter
At= pi*dt^2/4;
Ac= pi*dci^2/4; %[m^2] casing area
Avs=pi*dvs_i.^2/4; % velocity String area [m^2]
Ah=pi*(dci^2-dvs_o^2)/4;%hydraulic area [m^2]
theta=0;
rg= 8.4430e-006; % effective dy gas roughness [m];
% % %-----

% %-----Annulus part 1-----

%(2) Node2 to Node 3=> Annulus section

zan=[top_of_perforation:Velocity_String_Depth]; %% span of calculation

xan0=[x(end,1)-0.000001 %% Intial value for pressure ---x1
      vsg_0%% initial gas velocity ---x2
      x(end,1) %% initial reservoir pressure at the top-----x3
      x(end,2)]; %% Initial Temperature value at the top-----x4
%%---Algorithm for annulus section
%
[zan,xan] =ode45('annulus',zan,xan0);

%%-----inflow performance-----
vmvs_0= ((xw(end,2)*(1+R)*Ac)+(xan(end,2)*(1+R)*Ah)); %%massflow=
rho_m*vm*Area

% %%-----Velocity String-----

```

```

zvsspan=[Velocity_String_Depth top_of_perforation]; %% range of
calculation
xvs0=[xw(end,1);
      vmvs_0; %% initial mixture velocity
      xw(end,4)]; %% inlet Temperature for velocity string

[zvs,xvs] =ode45('Velocity_String',zvsspan,xvs0);
%-----
%-----Production tubing-----
vmtb_0= xvs(end,2)*Avs/At; %% initial mixture velocity for production
tubing
tubingspan=[top_of_perforation 0];%%----- range of calculation from
surface (0) to top of Perf.
tb0=[xvs(end,1); %%-----Initial pressure value
      vmtb_0; %% initial mixture velocity
      xvs(end,3)]; %% initial temperature
[ztb,xtb] =ode45('Tubing_String',tubingspan,tb0);%%-----the actual
computation

%-----Annulus function-----
function dxdz= annulus(z,x)

global g dh Ah Ma n Rg Z C rho1 Ah R

dxdz=zeros(4,1);

dxdz(1)= -(rho1(x)*g) +(fan(x)*vm(x)*abs(vm(x))/(2*dh));
dxdz(2)= qg(x)/Ah;%%
dxdz(3)= rrho1(x)*g; %% reservoir pressure dprdz
dxdz(4)= 0.02; %% temprature gradient

function gasdensity= rho1(x)

global Ma Rg Z

gasdensity= Ma*x(1)/(Rg*Z*x(4));

return
function reservoirdensity= rrho1(x)

global Ma Rg Z

reservoirdensity= Ma*x(3)/(Rg*Z*x(4));

return

function ed=r(x)

global R rg sigma

```

```

if R >= 0.007
    ed= (28.5*sigma/(0.3048*rhon(x)*vm(x)^2));

else
    ed= rg+ R*(((28.5*sigma/(0.3048*rhon(x)*vm(x)^2))-rg)/0.007);
end

function friction = fan(x)
global dh

friction = (1/(-1.8*log(6.9/Re(x) + (r(x)/(3.7*dh))^1.11))^2);

return

function kutaltelatze= kuan(x)

global g rhol sigma

% kutaltelatze number is used to determine If Gray has to be modified
or not
kutaltelatze = (sqrt(rhog(x))/(sigma*g*(rhol-rhog(x)))^0.25)*x(2);

function nonslipg = lambdag

global R

nonslipg= 1/(R+1);

function gasflowrate=qq(x)

global C n

gasflowrate=C*(x(3)^2-x(1)^2)^n;

function Reynolds= Re(x)

global miug miul dh

miun= lambdag*miug + (1-lambdag)*miul; % nonslip viscosity
% mium= alphag(x)*miug + (1-alphag(x))*miul; %% slip viscosity
Reynolds= rhon(x)*vm(x)*dh/miun; %% non-slip Reynolds number

function mixturevelocity= vm(x)

global R

mixturevelocity= x(2)*(1+R);

function nonslipdensity=rhon(x)

```

```

global rhol

nonslipdensity= (lambdag*rhog(x))+ ((1-lambdag)*rhol);

%-----Wellbore function-----

function dxdz= wellbore(z,x)

global g dci Ac

dpdz=(rhom(x)*g)+(fw(x)*rhom(x)*vm(x)^2/(2*dci)) ;

dxdz=zeros(4,1);
dxdz(1)= dpdz; %pressure gradient
dxdz(2)= -qg(x)/Ac; %% vsg gradient
dxdz(3)= rrhog(x)*g;
dxdz(4)= 0.02; %% temprature gradient

function gasvoid= alphag(x)

global g rhol dci theta R sigma

Nv=rhon(x)^2*vm(x)^4/(g*sigma*(rhol-rhog(x)));% nondimensional velocity
Nd=g*(rhol-rhog(x))*dci^2/sigma;% nondimensional diameter
B=-2.314*(Nv*(1+(205/Nd)))^(0.0814*(1-0.0554*log(1+(730*R/(R+1))))); %
a constant value supplied to alphag
vb= 0.345*sqrt(dci*g*(rhol-rhog(x))/rhol); % buble rise velocity
% vb=1.53*(g*(rhol-rhog(x))*sigma/rhol^2)^0.25

if ku(x)> 3.1*(1+0.31*sin(2*theta))% kutatelatze number, it determines
either Gray is modified or not

gasvoid=((1-exp(B))/(R+1));

else
    gasvoid =(((R+(-vb/x(2)))/(R+1+(vb/x(2)))));
end

function friction = fw(x)

global dci

friction = (1/(-1.8*log(6.9/Re(x) + (r(x)/(3.7*dci))^1.11))^2);

return

```

```

function kutaltelatze= ku(x)

global g rhol sigma

% kutaltelatze number is used to determine If Gray has to be modified
or not
kutaltelatze = (sqrt(rhog(x))/(sigma*g*(rhol-rhog(x)))^0.25)*x(2);

function nonslipg = lambdag

global R

nonslipg= 1/(R+1);

function gasflowrate=qg(x)
global n C
gasflowrate=C*((x(3)^2)-(x(1)^2))^n;

function ed=r(x)

global rg R sigma

if R >= 0.007
    ed= (28.5*sigma/(0.3048*rhom(x)*vm(x)^2));

else
    ed= rg+ R*(((28.5*sigma/(0.3048*rhom(x)*vm(x)^2))-rg)/0.007);
end

function Reynolds= Re(x)

global miug miul dci

mium= alphag(x)*miug + (1-alphag(x))*miul; %% %%mixture viscosity is
calculated in terms of gas hold up

Reynolds= rhom(x)*vm(x)*dci/mium;

function gasdensity= rhog(x)

global Ma Rg Z

gasdensity= Ma*x(1)/(Rg*Z*x(4));

function mixturedensity= rhom(x)

global rhol

mixturedensity= alphag(x)*rhog(x) +(1-alphag(x))*rhol;

```

```

function nonslipdensity=rhon(x)

global rhol

nonslipdensity= (lambdag*rhog(x))+ ((1-lambdag)*rhol);

function reservoirdensity= rrhog(x)

global Ma Rg Z

reservoirdensity= Ma*x(3)/(Rg*Z*x(4));

return

function mixturevelocity= vm(x)

global R Ac

mixturevelocity= x(2)*(1+R);

%-----Velocity string function-----

function dxdz= Velocity_String(z,x)

global g dvt Ma Rg Z rhol sigma R Avs

dvt=(rhom(x)*g)+(fvs(x)*rhom(x)*vm(x)^2/(2*dvt));
drhondz=lambdag*Ma*dvt/(Rg*Z*x(3));

dxdz=zeros(3,1);
dxdz(1)= dvt;
dxdz(2)=-(vm(x)/rhom(x))*drhondz; %%dvm/dz
dxdz(3)=0.02; %% dT/dz
%

function gasvoid= alphag(x)

global g sigma rhol dvt theta R Avs

delta_rho= rhol-rhog(x);
Nv= rhon(x)^2*vm(x)^4/(g*sigma*delta_rho);
Nd=g*delta_rho*dvt^2/sigma;
B=-2.314*(Nv*(1+(205/Nd)))^(0.0814*(1-0.554*log(1+(730*R/(R+1))))); % a
constant value supplied to alphag
vb= 0.345*sqrt(dvt*g*delta_rho/rhol); % bubble rise velocity

```

```

if ku(x)> 3.1*(1+0.31*sin(2*theta))%%%kutatelatze number, it determines
either Gray is modified or not

gasvoid= (1-exp(B))/(R+1);

else

    gasvoid =(((R+(-vb/vsg(x)))/(R+1+(vb/vsg(x)))));
end

function Reynolds= Re(x)

global miug miul dvsi

mium= alphag(x)*miug + (1-alphag(x))*miul;
% mium= lambdag*miug + (1-lambdag)*miul;

Reynolds= rhom(x)*vm(x)*dvsi/mium;

function mixturedensity= rhom(x)

global rhol

mixturedensity= (alphag(x)*rhog(x)) + ((1-alphag(x))*rhol);

function nonslipdensity= rhon(x)

global rhol

nonslipdensity= (lambdag*rhog(x)) + (1-lambdag)*rhol;

function friction = fvs(x)

global dvsi

friction = (1/(-1.8*log(6.9/Re(x) + (r(x)/(dvsi*3.7))^1.11))^2);

return

function ed=r(x)

global rg vsl sigma R Avs

if R >= 0.007
    ed= 28.5*sigma/(0.3048*rhom(x)*vm(x)^2);

```

```

else

ed= rg+ R*((28.5*sigma/(0.3048*rhom(x)*vm(x)^2))-rg)/0.007);
end

function kutaltelatze= ku(x)

global g rhol R sigma

kutaltelatze = (sqrt(rhog(x)/(sigma*g*(rhol-rhog(x)))^0.25))*vsg(x);

function superficialgas_velocity=vsg(x)

global R Avs

superficialgas_velocity= x(2);

function nonslipg = lambdag

global R

nonslipg= 1/(R+1);

function mixturevelocity= vm(x)

global Avs R

mixturevelocity= vsg(x)*(1+R);

function gasdensity= rhog(x)

global Ma Rg Z

gasdensity= Ma*x(1)/(Rg*Z*x(3));

function temprature= T(x)
temprature= x(3);

%-----TubingString function-----

function dxdz= Tubing_String(z,x)

global g dt Ma Rg Z rhol sigma R At

```

```

dpdz=(rhom(x)*g)+(fvs(x)*rhom(x)*vm(x)^2/(2*dt)) ;
drhondz=lambdag*Ma*dpdz/(Rg*Z*x(3));

dxdz=zeros(3,1);
dxdz(1)= dpdz;
dxdz(2)=-(vm(x)/rhom(x))*drhondz; %%dvm/dz
dxdz(3)=0.02; %% dT/dz

function gasvoid= alphag(x)

global g sigma rhol dt theta R At

delta_rho= rhol-rhog(x);
Nv= rhon(x)^2*vm(x)^4/(g*sigma*delta_rho);
Nd=g*delta_rho*dt^2/sigma;
B=-2.314*(Nv*(1+(205/Nd)))^(0.0814*(1-0.554*log(1+(730*R/(R+1))))); % a
constant value supplied to alphag
vb= 0.345*sqrt(dt*g*delta_rho/rhol); % buble rise velocity

if ku(x)> 3.1*(1+0.31*sin(2*theta))%%kutatelatze number, it determines
either Gray is modified or not

gasvoid= (1-exp(B))/(R+1);

else

    gasvoid =(((R+(-vb/vsg(x)))/(R+1+(vb/vsg(x)))));
end
% figure(1)
% plot(vg(x),gasvoid,'.')
% hold on
% xlabel('Vg')
% ylabel('alpha')
% grid on

function Reynolds= Re(x)

global miug miul dt

mium= alphag(x)*miug + (1-alphag(x))*miul;
% mium= lambdag*miug + (1-lambdag)*miul;

Reynolds= rhom(x)*vm(x)*dt/mium;

function mixturedensity= rhom(x)

global rhol

mixturedensity= (alphag(x)*rhog(x)) + ((1-alphag(x))*rhol);

```

```

function nonslipdensity= rhon(x)

global rhol

nonslipdensity= (lambdag*rhog(x)) + (1-lambdag)*rhol;

function friction = fvs(x)

global dt

friction = (1/(-1.8*log(6.9/Re(x) + (r(x)/(dt*3.7))^1.11))^2);

return

function ed=r(x)

global rg sigma R At

if R >= 0.007
    ed= 28.5*sigma/(0.3048*rhom(x)*vm(x)^2);
else
ed= rg+ R*((28.5*sigma/(0.3048*rhom(x)*vm(x)^2))-rg)/0.007);
end

function kutaltelatze= ku(x)

global g rhol R sigma

kutaltelatze = (sqrt(rhog(x)/(sigma*g*(rhol-rhog(x)))^0.25))*vsg(x);

function superficialgas_velocity=vsg(x)

global R At

superficialgas_velocity= x(2);

function nonslipg = lambdag

global R

nonslipg= 1/(R+1);

```

```
function mixturevelocity= vm(x)
```

```
global R
```

```
mixturevelocity= x(2)*(1+R);
```

```
function gasdensity= rhog(x)
```

```
global Ma Rg Z
```

```
gasdensity= Ma*x(1)/(Rg*Z*x(3));
```

```
function temprature= T(x)
```

```
temprature= x(3);
```